January 1973

Solving Three-Dimensional Potential Flow Problems by Means of an Inverse Formulation and Finite Differences

Allen L. Davis

Roland W. Jeppson

SOLVING THREE-DIMENSIONAL POTENTIAL FLOW PROBLEMS BY MEANS OF AN INVERSE FORMULATION AND FINITE DIFFERENCES

by

Allen L. Davis
and
Roland W. Jeppson

This research was carried out under the Naval Ship Systems Command
General Hydromechanics Research Program Subproject SR 009 01 01
administered by the Naval Ship Research and Development Center
Contract No. N00014-67-A-0220-0003

Utah Water Research Laboratory
College of Engineering
Utah State University
Logan, Utah 84322

March 1973

PRWG-96

SOLVING THREE-DIMENSIONAL POTENTIAL FLOW PROBLEMS BY MEANS OF AN INVERSE FORMULATION AND FINITE DIFFERENCES

by

Allen L. Davis
and
Roland W. Jeppson

This research was carried out under the Naval Ship Systems Command
General Hydromechanics Research Program Subproject SR 009 01 01
administered by the Naval Ship Research and Development Center
Contract No. N00014-67-A-0220-0003

Utah Water Research Laboratory
College of Engineering
Utah State University
Logan, Utah 84322

March 1973

PRWG-96-2

ABSTRACT

A finite difference method is developed to solve the three-dimensional, steady, incompressible, potential flow equations obtained by using a potential function, ϕ, and two mutually orthogonal stream functions, ψ and ψ^*, to describe the flow. Problems are formulated in an inverse space where the potential function and the two stream functions are the independent variables, and the Cartesian coordinates x, y, and z are the dependent variables. The boundaries of the problem in the physical space, including the free surface, have known positions in the inverse space, so trial and error adjustments to the positions of the boundaries are unnecessary.

Methods of describing the effect of the placement of a body, whose shape is partially specified, in the flow field are developed using finite differences, and a solution for the x-, y-, and z-coordinates is obtained at each grid point formed by the intersection of surfaces held constant with respect to ϕ, ψ, and ψ^* in the inverse space.

DEVELOPMENT OF THE THREE-DIMENSIONAL INVERSE EQUATIONS

Inverse transformation

The development of the three-dimensional inverse equations begins by using the chain rule to differentiate the functional relationships $\Phi = F(X,Y,Z)$, $\Psi = G(X,Y,Z)$, $\Psi^* = H(X,Y,Z)$ as follows:

$$\frac{\partial \Phi}{\partial \Phi} = \frac{\partial \Phi}{\partial X}\frac{\partial X}{\partial \Phi} + \frac{\partial \Phi}{\partial Y}\frac{\partial Y}{\partial \Phi} + \frac{\partial \Phi}{\partial Z}\frac{\partial Z}{\partial \Phi} = 1 \quad . \quad . \quad . \quad . \quad (9)$$

$$\frac{\partial \Psi}{\partial \Phi} = \frac{\partial \Psi}{\partial X}\frac{\partial X}{\partial \Phi} + \frac{\partial \Psi}{\partial Y}\frac{\partial Y}{\partial \Phi} + \frac{\partial \Psi}{\partial Z}\frac{\partial Z}{\partial \Phi} = 0 \quad . \quad . \quad . \quad . (10)$$

$$\frac{\partial \Psi^*}{\partial \Phi} = \frac{\partial \Psi^*}{\partial X}\frac{\partial X}{\partial \Phi} + \frac{\partial \Psi^*}{\partial Y}\frac{\partial Y}{\partial \Phi} + \frac{\partial \Psi^*}{\partial Z}\frac{\partial Z}{\partial \Phi} = 0 \quad . \quad . (11)$$

Equations 9, 10, and 11 result because the surfaces defined by holding Φ constant are orthogonal to the surfaces defined by holding Ψ and Ψ^* constant. Solving for $\partial X/\partial \Phi$, $\partial Y/\partial \Phi$, and $\partial Z/\partial \Phi$ by Cramer's rule (19) yields

$$\frac{\partial X}{\partial \Phi} = \frac{\begin{vmatrix} 1 & \frac{\partial \Phi}{\partial Y} & \frac{\partial \Phi}{\partial Z} \\ 0 & \frac{\partial \Psi}{\partial Y} & \frac{\partial \Psi}{\partial Z} \\ 0 & \frac{\partial \Psi^*}{\partial Y} & \frac{\partial \Psi^*}{\partial Z} \end{vmatrix}}{J} = \frac{\frac{\partial \Psi}{\partial Y}\frac{\partial \Psi^*}{\partial Z} - \frac{\partial \Psi}{\partial Z}\frac{\partial \Psi^*}{\partial Y}}{J} = \frac{u}{J} \quad . \quad . (12)$$

$$\frac{\partial Y}{\partial \Phi} = \frac{\begin{vmatrix} \frac{\partial \Phi}{\partial X} & 1 & \frac{\partial \Phi}{\partial Z} \\ \frac{\partial \Psi}{\partial X} & 0 & \frac{\partial \Psi}{\partial Z} \\ \frac{\partial \Psi^*}{\partial X} & 0 & \frac{\partial \Psi^*}{\partial Z} \end{vmatrix}}{J} = \frac{\frac{\partial \Psi}{\partial Z}\frac{\partial \Psi^*}{\partial X} - \frac{\partial \Psi}{\partial X}\frac{\partial \Psi^*}{\partial Z}}{J} = \frac{v}{J} \quad . \quad . (13)$$

$$\frac{\partial Z}{\partial \Phi} = \frac{\begin{vmatrix} \frac{\partial \Phi}{\partial X} & \frac{\partial \Phi}{\partial Y} & 1 \\ \frac{\partial \Psi}{\partial X} & \frac{\partial \Psi}{\partial Y} & 0 \\ \frac{\partial \Psi^*}{\partial X} & \frac{\partial \Psi^*}{\partial Y} & 0 \end{vmatrix}}{J} = \frac{\frac{\partial \Psi}{\partial X}\frac{\partial \Psi^*}{\partial Y} - \frac{\partial \Psi}{\partial Y}\frac{\partial \Psi^*}{\partial X}}{J} = \frac{w}{J} \quad . \quad . (14)$$

where J is the Jacobian given by the determinant

$$J = \begin{vmatrix} \frac{\partial \Phi}{\partial X} & \frac{\partial \Phi}{\partial Y} & \frac{\partial \Phi}{\partial Z} \\ \frac{\partial \Psi}{\partial X} & \frac{\partial \Psi}{\partial Y} & \frac{\partial \Psi}{\partial Z} \\ \frac{\partial \Psi^*}{\partial X} & \frac{\partial \Psi^*}{\partial Y} & \frac{\partial \Psi^*}{\partial Z} \end{vmatrix} = u^2 + v^2 + w^2 = V^2 \quad . \quad . (15)$$

The chain rule can also be employed to produce Eqs. 16 through 18.

$$\frac{\partial \Phi}{\partial \Phi} = \frac{\partial \Phi}{\partial X}\frac{\partial X}{\partial \Phi} + \frac{\partial \Phi}{\partial Y}\frac{\partial Y}{\partial \Phi} + \frac{\partial \Phi}{\partial Z}\frac{\partial Z}{\partial \Phi} = 1 \quad . \quad . (16)$$

$$\frac{\partial \Phi}{\partial \Psi} = \frac{\partial \Phi}{\partial X}\frac{\partial X}{\partial \Psi} + \frac{\partial \Phi}{\partial Y}\frac{\partial Y}{\partial \Psi} + \frac{\partial \Phi}{\partial Z}\frac{\partial Z}{\partial \Psi} = 0 \quad . \quad . (17)$$

$$\frac{\partial \Phi}{\partial \Psi^*} = \frac{\partial \Phi}{\partial X}\frac{\partial X}{\partial \Psi^*} + \frac{\partial \Phi}{\partial Y}\frac{\partial Y}{\partial \Psi^*} + \frac{\partial \Phi}{\partial Z}\frac{\partial Z}{\partial \Psi^*} = 0 \quad . \quad . (18)$$

Cramer's rule is used again to solve for $\partial \Phi/\partial X$, $\partial \Phi/\partial Y$, and $\partial \Phi/\partial Z$.

$$\frac{\partial \Phi}{\partial X} = \frac{\begin{vmatrix} 1 & \frac{\partial Y}{\partial \Phi} & \frac{\partial Z}{\partial \Phi} \\ 0 & \frac{\partial Y}{\partial \Psi} & \frac{\partial Z}{\partial \Psi} \\ 0 & \frac{\partial Y}{\partial \Psi^*} & \frac{\partial Z}{\partial \Psi^*} \end{vmatrix}}{j} = \frac{\frac{\partial Y}{\partial \Psi}\frac{\partial Z}{\partial \Psi^*} - \frac{\partial Z}{\partial \Psi}\frac{\partial Y}{\partial \Psi^*}}{j} = u \quad . \quad . (19)$$

$$\frac{\partial \Phi}{\partial Y} = \frac{\begin{vmatrix} \frac{\partial X}{\partial \Phi} & 1 & \frac{\partial Z}{\partial \Phi} \\ \frac{\partial X}{\partial \Psi} & 0 & \frac{\partial Z}{\partial \Psi} \\ \frac{\partial X}{\partial \Psi^*} & 0 & \frac{\partial Z}{\partial \Psi^*} \end{vmatrix}}{j} = \frac{\frac{\partial Z}{\partial \Psi}\frac{\partial X}{\partial \Psi^*} - \frac{\partial X}{\partial \Psi}\frac{\partial Z}{\partial \Psi^*}}{j} = v \quad . \quad . (20)$$

$$\frac{\partial \Phi}{\partial Z} = \frac{\begin{vmatrix} \frac{\partial X}{\partial \Phi} & \frac{\partial Y}{\partial \Phi} & 1 \\ \frac{\partial X}{\partial \Psi} & \frac{\partial Y}{\partial \Psi} & 0 \\ \frac{\partial X}{\partial \Psi^*} & \frac{\partial Y}{\partial \Psi^*} & 0 \end{vmatrix}}{j} = \frac{\frac{\partial X}{\partial \Psi}\frac{\partial Y}{\partial \Psi^*} - \frac{\partial Y}{\partial \Psi}\frac{\partial X}{\partial \Psi^*}}{j} = w \quad . . (21)$$

The inverse Jacobian determinant denoted by j, is

$$j = \begin{vmatrix} \frac{\partial X}{\partial \Phi} & \frac{\partial Y}{\partial \Phi} & \frac{\partial Z}{\partial \Phi} \\ \frac{\partial X}{\partial \Psi} & \frac{\partial Y}{\partial \Psi} & \frac{\partial Z}{\partial \Psi} \\ \frac{\partial X}{\partial \Psi^*} & \frac{\partial Y}{\partial \Psi^*} & \frac{\partial Z}{\partial \Psi^*} \end{vmatrix} \quad . . . . . (22)$$

Equating the velocity components u, v, and w from Eqs. 12 and 19, 13 and 20, and 14 and 21 produces the inverse equations

$$u = J\frac{\partial X}{\partial \Phi} = \frac{1}{j}\left(\frac{\partial Y}{\partial \Psi}\frac{\partial Z}{\partial \Psi^*} - \frac{\partial Z}{\partial \Psi}\frac{\partial Y}{\partial \Psi^*}\right) \quad . . . . . (23)$$

$$v = J\frac{\partial Y}{\partial \Phi} = \frac{1}{j}\left(\frac{\partial Z}{\partial \Psi}\frac{\partial X}{\partial \Psi^*} - \frac{\partial X}{\partial \Psi}\frac{\partial Z}{\partial \Psi^*}\right) \quad . . . . . (24)$$

$$w = J\frac{\partial Z}{\partial \Phi} = \frac{1}{j}\left(\frac{\partial X}{\partial \Psi}\frac{\partial Y}{\partial \Psi^*} - \frac{\partial Y}{\partial \Psi}\frac{\partial X}{\partial \Psi^*}\right) \quad . . . . . (25)$$

but since $J = 1/j$ the equations reduce to

$$\frac{\partial X}{\partial \Phi} = \frac{\partial Y}{\partial \Psi}\frac{\partial Z}{\partial \Psi^*} - \frac{\partial Z}{\partial \Psi}\frac{\partial Y}{\partial \Psi^*} \quad . . . . . (26)$$

$$\frac{\partial Y}{\partial \Phi} = \frac{\partial Z}{\partial \Psi}\frac{\partial X}{\partial \Psi^*} - \frac{\partial X}{\partial \Psi}\frac{\partial Z}{\partial \Psi^*} \quad . . . . . (27)$$

$$\frac{\partial Z}{\partial \Phi} = \frac{\partial X}{\partial \Psi}\frac{\partial Y}{\partial \Psi^*} - \frac{\partial Y}{\partial \Psi}\frac{\partial X}{\partial \Psi^*} \quad . . . . . (28)$$

Nondimensionalization of the equations

In utilizing the results from solutions, it is desirable to work with inverse equations that are dimensionless in both dependent and independent variables. The potential function has dimensions of (ft^2/sec), which dimensions are the same as those of the two-dimensional potential function. From Eq. 5 the dimensions of the velocity component u must match those of $(\partial\Psi/\partial Y)$ $(\partial\Psi^*/\partial Z)$, so Ψ and Ψ^* must have dimensions of ($\sqrt{ft^3/sec}$). The dimensionless potential function ϕ will be defined by

$$\phi = \Phi\left(\frac{NP1}{Q/W}\right) \quad . . . . . (29)$$

in which Q is the flow rate (ft^3/sec), W is a characteristic width of flow, which in the problem described later will be the channel width (ft), and NP1 is one less than the number of equipotential surfaces, which will constitute grid planes to be used in the finite difference solution described later. The dimensionless stream functions ψ and ψ^* will be defined by

$$\psi = \Psi\left(\frac{NS1}{\sqrt{Q}}\right) \quad . . . . . (30)$$

$$\psi^* = \Psi^*\left(\frac{NSS1}{\sqrt{Q}}\right) \quad . . . . . (31)$$

where NS1 and NSS1 are one less than the number of ψ and ψ^* grid planes, respectively. The chain rule of differentiation gives

$$\frac{\partial X}{\partial \Phi} = \frac{\partial X}{\partial \phi}\frac{\partial \phi}{\partial \Phi} = w\left(\frac{NP1}{Q}\right)\frac{\partial X}{\partial \phi} \quad . . . . . (32)$$

$$\frac{\partial Y}{\partial \Psi} = \frac{\partial Y}{\partial \psi}\frac{\partial \psi}{\partial \Psi} = \frac{NS1}{\sqrt{Q}}\frac{\partial Y}{\partial \psi} \quad . . . . . (33)$$

$$\frac{\partial Y}{\partial \Psi^*} = \frac{\partial Y}{\partial \psi^*}\frac{\partial \psi^*}{\partial \Psi^*} = \frac{NSS1}{\sqrt{Q}}\frac{\partial Y}{\partial \psi^*} \quad . . . . . (34)$$

$$\frac{\partial Z}{\partial \Psi^*} = \frac{\partial Z}{\partial \psi^*}\frac{\partial \psi^*}{\partial \Psi^*} = \frac{NSS1}{\sqrt{Q}}\frac{\partial Z}{\partial \psi^*} \quad . . . . . (35)$$

$$\frac{\partial Z}{\partial \Psi} = \frac{\partial Z}{\partial \psi}\frac{\partial \psi}{\partial \Psi} = \frac{NS1}{\sqrt{Q}}\frac{\partial Z}{\partial \psi} \quad . . . . . (36)$$

Substituting Eqs. 32 through 36 into Eq. 26 produces

$$w\left(\frac{NP1}{Q}\right)\frac{\partial X}{\partial \phi} = \frac{(NS1)\ (NSS1)}{Q}\left[\frac{\partial Y}{\partial \psi}\frac{\partial Z}{\partial \psi^*} - \frac{\partial Z}{\partial \psi}\frac{\partial Y}{\partial \psi^*}\right] \quad . . . . . (37)$$

Similarly,

$$w\left(\frac{NP1}{Q}\right)\frac{\partial Y}{\partial \phi} = \frac{(NS1)\ (NSS1)}{Q}\left[\frac{\partial Z}{\partial \psi}\frac{\partial x}{\partial \psi^*} - \frac{\partial X}{\partial \psi}\frac{\partial Z}{\partial \psi^*}\right] \quad . . . . . (38)$$

$$w\left(\frac{NP1}{Q}\right)\frac{\partial Z}{\partial \phi} = \frac{(NS1)\ (NSS1)}{Q}\left[\frac{\partial X}{\partial \psi}\frac{\partial Y}{\partial \psi^*} - \frac{\partial Y}{\partial \psi}\frac{\partial X}{\partial \psi^*}\right] \quad . . . . . (39)$$

The dependent variables X, Y, and Z will be made dimensionless by dividing by the characteristic width of flow, i.e.

$$x = X/W \quad \ldots\ldots\ldots\ldots\ldots\ldots (40)$$

$$y = Y/W \quad \ldots\ldots\ldots\ldots\ldots\ldots (41)$$

$$z = Z/W \quad \ldots\ldots\ldots\ldots\ldots\ldots (42)$$

Then

$$\frac{\partial X}{\partial \phi} = \frac{\partial X}{\partial x}\frac{\partial x}{\partial \phi} = W\frac{\partial x}{\partial \phi} \quad \ldots\ldots\ldots\ldots (43)$$

$$\frac{\partial X}{\partial \psi} = W\frac{\partial x}{\partial \psi} \quad \ldots\ldots\ldots\ldots\ldots (44)$$

$$\frac{\partial X}{\partial \psi^*} = W\frac{\partial x}{\partial \psi^*} \quad \ldots\ldots\ldots\ldots\ldots (45)$$

$$\frac{\partial Y}{\partial \phi} = W\frac{\partial y}{\partial \phi} \quad \ldots\ldots\ldots\ldots\ldots (46)$$

$$\frac{\partial Y}{\partial \psi} = W\frac{\partial y}{\partial \psi} \quad \ldots\ldots\ldots\ldots\ldots (47)$$

$$\frac{\partial Y}{\partial \psi^*} = W\frac{\partial y}{\partial \psi^*} \quad \ldots\ldots\ldots\ldots\ldots (48)$$

$$\frac{\partial Z}{\partial \phi} = W\frac{\partial z}{\partial \phi} \quad \ldots\ldots\ldots\ldots\ldots (49)$$

$$\frac{\partial Z}{\partial \psi} = W\frac{\partial z}{\partial \psi} \quad \ldots\ldots\ldots\ldots\ldots (50)$$

$$\frac{\partial Z}{\partial \psi^*} = W\frac{\partial z}{\partial \psi^*} \quad \ldots\ldots\ldots\ldots\ldots (51)$$

Substituting Eqs. 43 through 51 into Eqs. 37 through 39 and defining C as

$$C = \frac{NP1}{(NS1)\ (NSS1)} \quad \ldots\ldots\ldots\ldots\ldots (52)$$

produces the following dimensionless inverse equations:

$$C\frac{\partial x}{\partial \zeta} = \frac{\partial y}{\partial \psi}\frac{\partial z}{\partial \psi^*} - \frac{\partial z}{\partial \psi}\frac{\partial y}{\partial \psi^*} \quad \ldots\ldots\ldots\ldots (53)$$

$$C\frac{\partial y}{\partial \zeta} = \frac{\partial z}{\partial \psi}\frac{\partial x}{\partial \psi^*} - \frac{\partial x}{\partial \psi}\frac{\partial z}{\partial \psi^*} \quad \ldots\ldots\ldots\ldots (54)$$

$$C\frac{\partial z}{\partial \zeta} = \frac{\partial x}{\partial \psi}\frac{\partial y}{\partial \psi^*} - \frac{\partial y}{\partial \psi}\frac{\partial x}{\partial \psi^*} \quad \ldots\ldots\ldots\ldots (55)$$

For two-dimensional flow, Eqs. 53 through 55 reduce to

$$C'\frac{\partial x}{\partial \zeta} = \frac{\partial y}{\partial \psi} \quad \ldots\ldots\ldots\ldots\ldots (56)$$

$$C'\frac{\partial y}{\partial \phi} = \frac{\partial x}{\partial \psi} \quad \ldots\ldots\ldots\ldots\ldots (57)$$

in which

$$C' = \frac{NP1}{NS1} \quad \ldots\ldots\ldots\ldots\ldots (58)$$

Equations 56 and 57 are the dimensionless forms of Eqs. 3 and 4.

Although Eqs. 26 through 28 and Eqs. 53 through 55 appear similar in form to Eqs. 3 and 4, and Eqs. 56 and 57, they cannot be combined into second order equations with one dependent variable as can be done for the equations for two dimensional flow. Equations 53, 54, and 55 are first order, nonlinear, partial differential equations, and in obtaining a solution, the boundary value problems associated with them must be solved simultaneously.

DESCRIPTION OF THE PHYSICAL AND SOLUTION SPACES

In order to simplify the placement of the physical space into the inverse space, the flows considered herein will be confined to those occurring in rectangular channels with horizontal bottoms. For such flows, $\psi = 0$ can be assigned to coincide with the channel bottom and $\psi = \psi_f$ (constant) to the free surface of the fluid. The left vertical wall, when facing downstream, will be assigned a value $\psi^* = 0$, and the opposite (right) vertical wall will be assigned a value $\psi^* = \psi_f^*$. At a section upstream from the flow of interest, ϕ will be assigned the value zero, and at the downstream boundary of interest ϕ will be denoted by the value ϕ_f. In defining the region in this manner, it will be assumed that the upstream and downstream boundaries are far enough removed from the phenomena of interest that uniform flow exists at these ϕ equal constant planes. This placement of the flow boundaries in the inverse solution space provides for a direct correspondence between the independent ϕ, ψ, and ψ^* variables and the dependent x, y, and z variables, as shown in Figure 1. When uniform flow exists, x increases linearly with ϕ in the direction of flow, y increases linearly with ψ, and z increases linearly with ψ^*.

When the flow deviates only slightly from uniform flow, this same general correspondence between variables exists throughout most of the flow field. In these regions, the magnitudes of the partial derivatives $\partial x/\partial\phi$, $\partial y/\partial\psi$, and $\partial z/\partial\psi^*$ will be approximately equal to 1/NP1, 1/NS1, and 1/NSS1, respectively, and the magnitude of the remaining derivatives in Eqs. 53 through 55 will not differ greatly from zero except where there is significant curvature of the streamlines.

In forming the finite difference grid network, NP equipotential surfaces, NS ψ constant stream surfaces, and NSS ψ^* constant stream surfaces will be used. The placement in the inverse space of bodies around which flow occurs will be accomplished by specifying the ψ and ψ^* constant surfaces that envelope the bodies and the equipotential surfaces that are coincident with the upstream and downstream stagnation points.

The body is collapsed onto a single line in the inverse space, with MB and NB denoting the enclosing ψ and ψ^* constant stream surfaces and LB and LN denoting the forward and rear equipotential surfaces that contain the stagnation points on the body. (See Figures 2, 10, and 11.)

The channel width W, uniform flow depth D, and the total head, $H = D + V^2/2g$, are specified for each problem. Other parameters associated with the flow, such as the uniform flow velocity, are determined from these specified parameters.

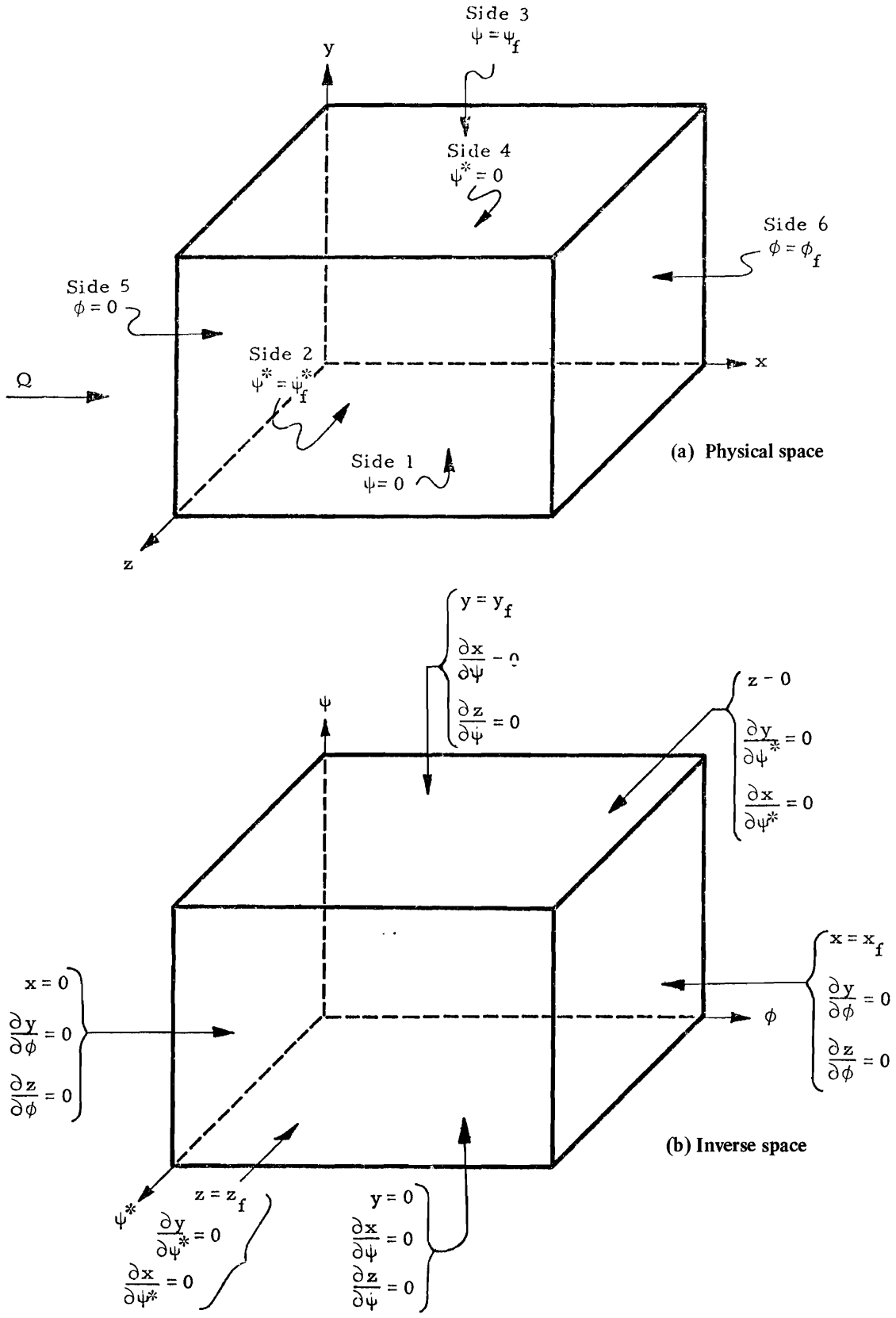

Figure 1. Coordinate systems and boundary conditions for a rectangular channel in the physical and inverse spaces.

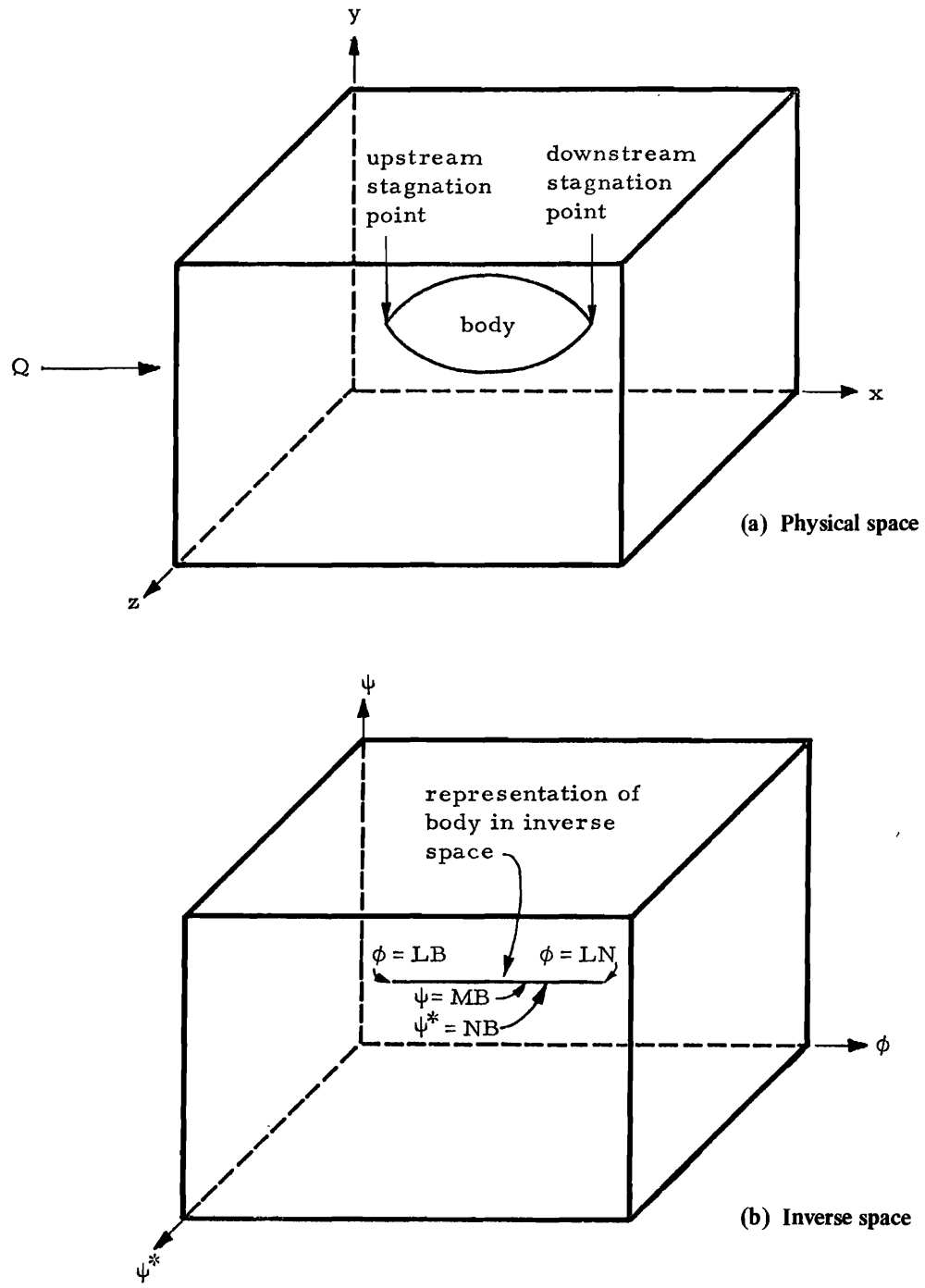

Figure 2. Illustration of the formulation of the problem of flow around a three-dimensional body in a rectangular channel in (a) the physical space and (b) the inverse space.

FINITE DIFFERENCE METHODS

The use of finite differences in solving elliptic, linear, partial differential equations results in a system of algebraic equations, expressed in matrix notation as

$$A\overline{U} = \overline{B} \quad \ldots\ldots\ldots\ldots\ldots\ldots (59)$$

where A is the matrix of coefficients in the system of equations, $\overline{U}$ is the vector of unknown quantities, and $\overline{B}$ is the vector of known quantities. This system of equations can be solved by direct matrix methods, such as Gaussian or Gauss-Jordan elimination, but for large matrices the capacity of the computer is soon exceeded, so iterative procedures are frequently used.

Commonly used iterative methods include the following (see Forsythe and Wasow (3)): the method of simultaneous displacements, or the Point Jacobi method; the method of successive displacements, or the Gauss-Seidel method; the successive overrelaxation method (SOR), which incorporates an overrelaxation factor into the Gauss-Seidel method to speed the rate of convergence of the solution; the line successive overrelaxation method (LSOR), which is similar to the SOR method except a whole block or line of unknowns is solved at once. The general convergence criteria for these iterative methods is that the matrix A be irreducible and have diagonal dominance (24), i.e., the sum of the absolute values of the off diagonal elements in any row must be less than or equal to and in at least one case be less than the absolute value of the diagonal element. This criteria can be interpreted to mean that the unknown being solved for has as much or more influence on the equation as the sum of all the other unknowns involved in that equation.

These iterative methods must be modified when applied to Eqs. 53 through 55, because the equations are nonlinear and the dependent variables can't be isolated one at a time in a first or second order equation involving the independent variables. Therefore, x, y, and z must be solved for simultaneously.

SUCCESSIVE PLANE RELAXATION METHOD

A method for solving the three-dimensional inverse equations that was studied initially consisted of solving for the dependent variables x, y, and z at each grid point on a single stream surface by direct methods under the assumption that the values on adjacent stream surfaces were known. This approach was finally abandoned but is described here to give the reader a better understanding concerning the difficulties in obtaining a solution. This approach represents an extension of the block or line successive relaxation methods described by Ames (1), Varga (24), and Forsythe and Wasow (7). Instead of solving for the dependent variables at all grid points along a line, the dependent variables are computed for all grid points on an entire ψ constant plane simultaneously. The dependent variables in each plane are solved for successively until all planes have been evaluated (see Figure 3). This process is repeated iteratively until the values of the dependent variables do not change significantly between successive passes through the planes. The above iterative approach to a solution will be referred to as the "successive plane relaxation method."

If the stream surfaces are taken as successive ψ constant planes such that derivatives with respect to ψ are assumed known temporarily, then Eqs. 53, 54, and 55 become:

$$C\frac{\partial x}{\partial \phi} = C2\frac{\partial z}{\partial \psi^*} - C3\frac{\partial y}{\partial \psi^*} \quad \ldots\ldots\ldots (60)$$

$$C\frac{\partial y}{\partial \phi} = C3\frac{\partial x}{\partial \psi^*} - C1\frac{\partial z}{\partial \psi^*} \quad \ldots\ldots\ldots (61)$$

$$C\frac{\partial z}{\partial \phi} = C1\frac{\partial y}{\partial \psi^*} - C2\frac{\partial x}{\partial \psi^*} \quad \ldots\ldots\ldots (62)$$

Equations 60, 61, and 62 would be linear if the C1, C2, and C3's were known constants. Thus, to form quasi-linear equations, the C1, C2, and C3's will be assumed to be constant while obtaining the solution on any plane (the j^{th} ψ constant plane) and will be approximated by central differences so no x, y, or z value from the j^{th} plane appears in the approximations. When second order central differences are used to determine values for the constants C1, C2, and C3,

$$C1 = \frac{\partial x}{\partial \psi} = \frac{0.5}{\Delta\psi}\left(x_{ij+1k} - x_{ij-1k}\right) \quad \ldots\ldots (63)$$

$$C2 = \frac{\partial y}{\partial \psi} = \frac{0.5}{\Delta\psi}\left(y_{ij+1k} - y_{ij-1k}\right) \quad \ldots\ldots (64)$$

$$C3 = \frac{\partial z}{\partial \psi} = \frac{0.5}{\Delta\psi}\left(z_{ij+1k} - z_{ij-1k}\right) \quad \ldots\ldots (65)$$

in which the subscripts i, j, and k are given by

$$i = 1 + \phi/\Delta\phi \quad \ldots\ldots\ldots\ldots\ldots (66)$$

$$j = 1 + \psi/\Delta\psi \quad \ldots\ldots\ldots\ldots\ldots (67)$$

$$k = 1 + \psi^*/\Delta\psi^* \quad \ldots\ldots\ldots\ldots\ldots (68)$$

This procedure linearizes the otherwise nonlinear equations while solving for the dependent variables on any plane and permits all the unknowns in this plane to be solved for simultaneously using matrix methods.

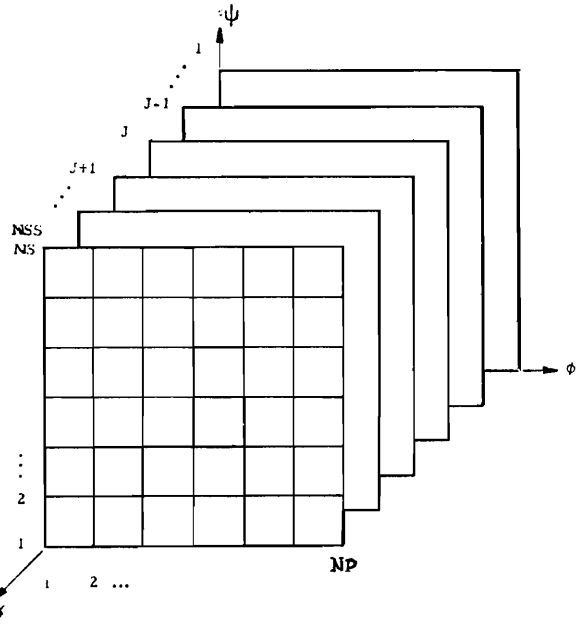

Figure 3. Plane structure of the finite difference network used in the "successive plane relaxation" method.

Third order forward and backward differences were used to approximate the derivatives with respect to ϕ and ψ^* in Eqs. 60, 61, and 62 at each grid point. Forward differences were used until the index associated with the independent variable appearing in the derivative reached half its final value, and backward differences were used thereafter. The matrix obtained by writing Eqs. 60, 61, and 62 in finite difference form at each grid point in a ψ constant plane appears in Figure 4.

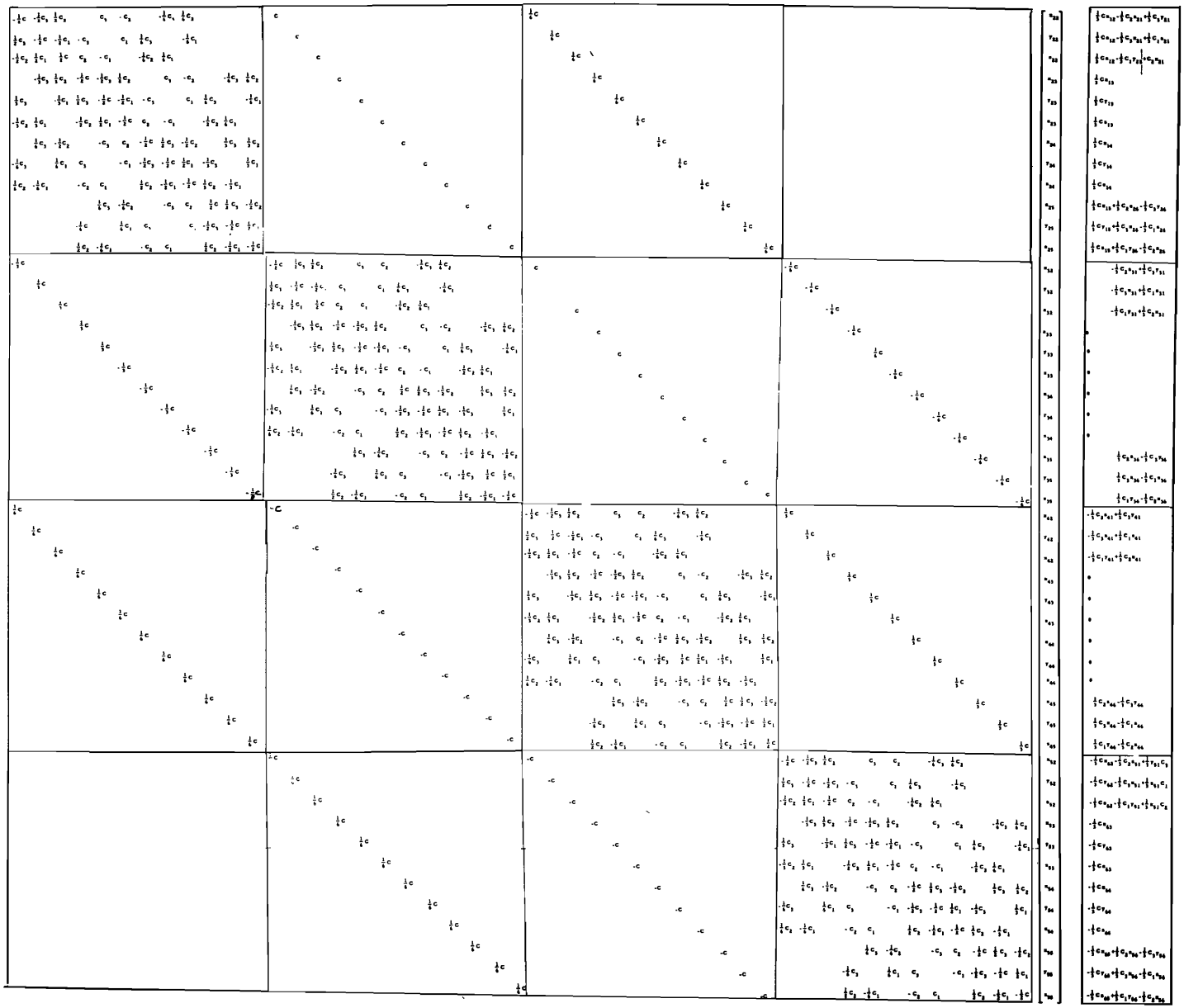

Figure 4. Matrix for obtaining x, y, and z for each grid point on a ψ constant plane assuming adjacent planes and boundary values are known.

An algorithm that utilizes the band properties of the matrix was used to conserve computer time and storage requirements and to minimize truncation error. Two algorithms were studied for solving the nonsymmetric band matrix without storing the zeroes above and below the band. One of these followed the procedure described by Thurnau (23) and took advantage of the bands. The other algorithm partitioned the matrix and used an elimination method similar to that described by Wilson (26).

The performance of the successive plane relaxation method was tested by introducing errors into the interior grid points of uniform flow and specifying the boundary values. A correct solution for x, y, and z in the j^{th} plane was obtained when the correct values for these variables were used in the j-1 and j+1 ψ constant planes. The correct solution indicated that the equations and algorithms were properly implemented in writing the computer program. However, when errors were introduced into the dependent variables at a single grid point in the j-1 ψ constant plane, divergence occurred initially, apparently until the introduced error had spread to surrounding grid points, but then converged rapidly to the correct solution. When such small errors were introduced at several interior grid points in adjacent j-1 and j+1 ψ constant planes, divergence continued from the proper values, with some x, y, and z variables becoming negative and some becoming larger than the largest boundary values. Constraints were placed on the variables, which required that they be nonnegative and less than the largest boundary value, but even under these constraints the successive plane relaxation method failed to converge.

Several things were attempted to cause convergence. For example, alternative differences were used for the derivatives with respect to ψ that brought values of x, y, and z from the j^{th} ψ constant plane into C1, C2, and C3, rather than to evaluate these coefficients entirely from adjacent planes. The x, y, and z values on the j^{th} plane were first considered known from the previous iteration, which allowed Eqs. 60, 61, and 62 to be treated as linear, and the equations were solved as before. The process still did not converge to the correct solution. Next, the dependent variables in the j^{th} plane were treated as unknowns, making Eqs. 60 through 62 nonlinear. The nonlinear system of equations was solved using the Newton-Raphson method. The solution by the Newton-Raphson method used the iterative equation

$$\bar{x}^{t+1} = \bar{x}^{t} - \overline{CV} \quad \ldots\ldots\ldots\ldots (69)$$

in which

$$\overline{CV} = D^{-1}\,\overline{F_t}\,(x) \quad \ldots\ldots\ldots\ldots (70)$$

$$D = \begin{bmatrix} \frac{\partial F1}{\partial x_{2,2,2}} & \frac{\partial F1}{\partial y_{2,2,2}} & \frac{\partial F1}{\partial z_{2,2,2}} & \frac{\partial F1}{\partial x_{2,2,3}} & \frac{\partial F1}{\partial y_{2,2,3}} & \frac{\partial F1}{\partial z_{2,2,3}} \cdots & \frac{\partial F1}{\partial x_{NP1,NS1,NSS1}} & \frac{\partial F1}{\partial y_{NP1,NS1,NSS1}} & \frac{\partial F1}{\partial z_{NP1,NS1,NSS1}} \\ \frac{\partial F2}{\partial x_{2,2,2}} & \frac{\partial F2}{\partial y_{2,2,2}} & \frac{\partial F2}{\partial z_{2,2,2}} & \frac{\partial F2}{\partial x_{2,2,3}} & \frac{\partial F2}{\partial y_{2,2,3}} & \frac{\partial F2}{\partial z_{2,2,3}} \cdots & \frac{\partial F2}{\partial x_{NP1,NS1,NSS1}} & \frac{\partial F2}{\partial y_{NP1,NS1,NSS1}} & \frac{\partial F2}{\partial z_{NP1,NS1,NSS1}} \\ \vdots & & & & & & & & \\ \frac{\partial Fn}{\partial x_{2,2,2}} & \frac{\partial Fn}{\partial y_{2,2,2}} & \frac{\partial Fn}{\partial z_{2,2,2}} & \frac{\partial Fn}{\partial x_{2,2,3}} & \frac{\partial Fn}{\partial y_{2,2,3}} & \frac{\partial Fn}{\partial z_{2,2,3}} \cdots & \frac{\partial Fn}{\partial x_{NP1,NS1,NSS1}} & \frac{\partial Fn}{\partial y_{NP1,NS1,NSS1}} & \frac{\partial Fn}{\partial z_{NP1,NS1,NSS1}} \end{bmatrix} \quad \ldots\ldots (71)$$

The elements of the vector $\overline{F}$ are

$$F1 = C\frac{\partial x}{\partial \phi} - (FAC2_{2,2,2} + FR\ y_{2,2,2})\frac{\partial z}{\partial \psi^*} + (FAC3_{2,2,2} + FR\ z_{2,2,2})\frac{\partial y}{\partial \psi^*}$$

$$F2 = C\frac{\partial y}{\partial \phi} - (FAC3_{2,2,2} + FR\ z_{2,2,2})\frac{\partial x}{\partial \psi^*} + (FAC1_{2,2,2} + FR\ x_{2,2,2})\frac{\partial z}{\partial \psi^*}$$

$$F3 = C\frac{\partial z}{\partial \phi} - (FAC1_{2,2,2} + FR\ x_{2,2,2})\frac{\partial y}{\partial \psi^*} + (FAC2_{2,2,2} + FR\ y_{2,2,2})\frac{\partial x}{\partial \psi^*}$$

$$F4 = C\frac{\partial x}{\partial \phi} - (FAC2_{2,2,3} + FR\ y_{2,2,3})\frac{\partial z}{\partial \psi^*} + (FAC3_{2,2,3} + FR\ z_{2,2,3})\frac{\partial y}{\partial \psi^*}$$

$$Fn = C\frac{\partial z}{\partial \phi} - (FAC1_{NP1,NS1,NSS1} + FR\ x_{NP1,NS1,NSS1})\frac{\partial y}{\partial \psi^*} + (FAC2_{NP1,NS1,NSS1} + FR\ y_{NP1,NS1,NSS1})\frac{\partial x}{\partial \psi^*}$$

in which FR is the coefficient from the finite difference operator that multiplies the unknown variable in the j^{th} plane, and FAC1, FAC2, and FAC3 include all other terms from adjacent ψ constant planes for the derivatives $\partial x/\partial \psi$, $\partial y/\partial \psi$, and $\partial z/\partial \psi$, respectively, which are used in the finite difference operators.

The derivative matrix has its entries in the same positions as the entries in the linear system of equations (see Figure 5, and compare with Figure 4), so the same algorithms were used to obtain the correction vector as were used to solve the linear system of equations in a plane.

An extremely good initialization was needed for the Newton-Raphson method to converge for a single ψ constant plane, but even when such an initialization was supplied, the process did not converge in iterating between planes.

An attempt was made to determine if fixing the derivatives with respect to ψ^*, so C1, C2, and C3 were the derivatives $\partial x/\partial \psi^*$, $\partial y/\partial \psi^*$, and $\partial z/\partial \psi^*$, respectively, would make the method convergent, but implementing this procedure proved unsuccessful also.

To insure that the variables at a grid point were not influenced more by surrounding values in a ψ constant plane than in a ψ^* constant plane, or vice versa, an alternating direction method was tried where the derivatives with respect to ψ were fixed on one iteration, and the derivatives with respect to ψ^* were fixed on the next, but convergence between planes again did not occur when the procedure was implemented on the computer.

The reasons why the plane successive relaxation method does not converge when point by point methods, as described next, converge are not apparent.

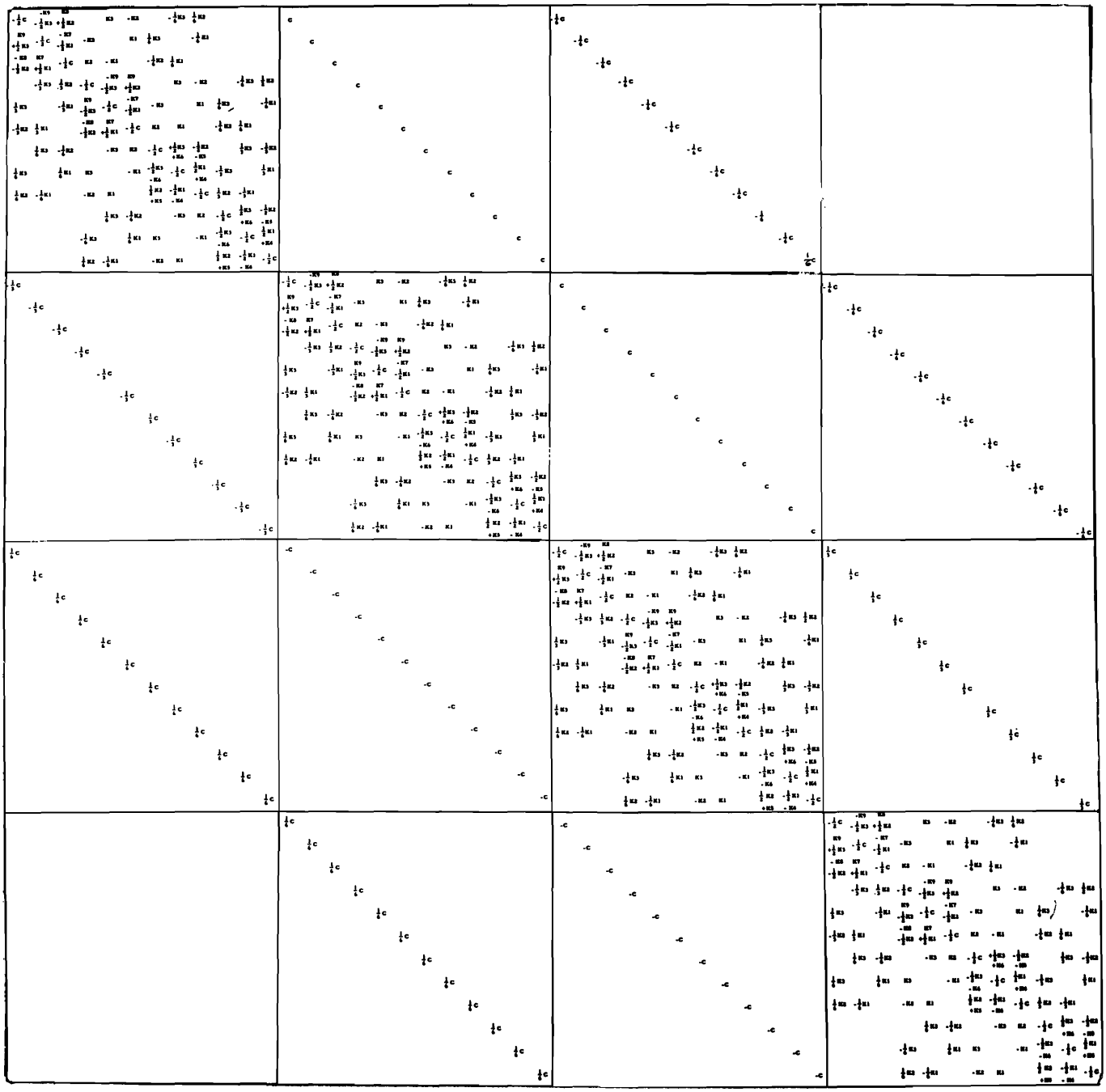

Figure 5. Derivative matrix for n-dimensional Newton-Raphson method.

MODIFIED GAUSS-SEIDEL METHOD

The method that was finally developed as a possible approach to solve boundary value problems associated with the nonlinear inverse Eqs. 53 through 55, is an extension of the Gauss-Seidel method. It will be referred to as the modified Gauss-Seidel method. The unknown variables x, y, and z at each grid point are solved for by assuming the variables at the surrounding grid points are known. The difference equations that result from this assumption are nonlinear and consist of three separate equations which must be solved simultaneously for the three unknowns x_{ijk}, y_{ijk}, and z_{ijk}. Since these equations are nonlinear, such criteria as diagonal dominance, which are commonly used to examine whether an iterative method will converge or not, cannot be examined per se. Because the difference equations consist of only first order derivatives, it is clear, however, that a point by point iterative scheme will converge only if first order differences are used. Finite difference operators resulting from second and higher order approximations do not have the equivalence of diagonal dominance. To illustrate, consider the following first and third order forward difference approximations

$$\frac{\partial x}{\partial \phi} \simeq \frac{x_{i+1jk} - x_{ijk}}{\Delta\phi} \quad \underline{1st}\ \text{order}$$

$$\simeq \frac{-\frac{1}{3}x_{i-1jk} - \frac{1}{2}x_{ijk} + x_{i+1jk} - \frac{1}{6}x_{i+2jk}}{\Delta\phi} \quad \underline{3rd}\ \text{order} \quad . \quad . \quad . (72)$$

The absolute value of the coefficient of the variable x_{ijk} equals the absolute value of the coefficient of the neighboring variable x_{i+1jk} when first order differences are used, but the absolute value of the coefficient of the variable x_{ijk} is less than the sum of the absolute values of the coefficients of the neighboring variables x_{i-1jk}, x_{i+1jk}, and x_{i+2jk} when third order differences are used. Use of a central difference eliminates the term x_{ijk} from the difference approximation.

There are eight possible combinations of first order forward and backward differences that can be used to approximate the inverse Eqs. 53, 54, and 55. Denoting forward differences by F and backward differences by B, these combinations are: FFF, FFB, FBF, FBB, BFF, BFB, BBF, and BBB, in which the first letter indicates differences with respect to ϕ, the second letter with respect to ψ, and the third letter with respect to ψ^*.

The FFF difference of Eq. 53 is,

$$C[x_{i+1jk} - x_{ijk}] = \frac{\Delta\phi}{\Delta\psi\ \Delta\psi^*}\{[y_{ij+1k} - y_{ijk}][z_{ijk+1} - z_{ijk}] - [z_{ij+1k} - z_{ijk}][y_{ijk+1} - y_{ijk}]\} \quad . \quad . \quad . (73)$$

If $\Delta\phi = \Delta\psi = \Delta\psi^* = 1$ and $R = 1/C$, Eq. 73 becomes

$$\begin{aligned} x_{ijk} &= x_{i+1jk} - R[y_{ij+1k}z_{ijk+1} - y_{ij+1k}z_{ijk} - z_{ijk+1}y_{ijk} \\ &\quad + y_{ijk}z_{ijk} - y_{ijk+1}z_{ij+1k} + y_{ijk+1}z_{ijk} + z_{ij+1k}y_{ijk} \\ &\quad - y_{ijk}z_{ijk}] \\ &= x_{i+1jk} - R[y_{ij+1k}z_{ijk+1} - y_{ij+1k}z_{ijk} - z_{ijk+1}y_{ijk} \\ &\quad - y_{ijk+1}z_{ij+1k} + y_{ijk+1}z_{ijk} + z_{ij+1k}y_{ijk}] \quad . \quad . (74) \end{aligned}$$

Note that the nonlinear term $y_{ijk}\ z_{ijk}$ drops out of Eq. 74, leaving a linear equation involving the three unknowns x_{ijk}, y_{ijk}, and z_{ijk}.

The FFF finite difference forms of Eqs. 54 and 55 are,

$$y_{ijk} = y_{i+1jk} - R[x_{ijk+1}z_{ij+1k} - x_{ijk+1}z_{ijk} - z_{ij+1k}x_{ijk} - x_{ij+1k}z_{ijk+1} + x_{ij+1k}z_{ijk} + z_{ijk+1}x_{ijk}]. \quad . (75)$$

and

$$z_{ijk} = z_{i+1jk} - R[x_{ij+1k}y_{ijk+1} - x_{ij+1k}y_{ijk} - y_{ijk+1}x_{ijk} - x_{ijk+1}y_{ij+1k} + x_{ijk+1}y_{ijk} + y_{ij+1k}x_{ijk}]. \quad . (76)$$

Since all but the terms x_{ijk}, y_{ijk}, and z_{ijk} are considered known temporarily, Eqs. 74, 75, and 76 constitute three linear equations with three unknowns at each grid point, which can be solved by matrix methods. These equations can be written in the form

$$\begin{aligned} a_{11}x + a_{12}y + a_{13}z &= b_1 \\ a_{21}x + a_{22}y + a_{23}z &= b_2 \\ a_{31}x + a_{32}y + a_{33}z &= b_3 \quad . \quad . \quad . \quad . \quad . \quad . \quad . \quad . \quad . (77) \end{aligned}$$

or

$$A\overline{U} = \overline{B} \quad . \quad . \quad . \quad . \quad . \quad . \quad . \quad . \quad . \quad . \quad . \quad . \quad . \quad . \quad . \quad . (78)$$

The A matrix depends upon which of the eight possible combinations of forward and backward differences are used, as given in Table 1.

Table 1. All possible combinations of first order forward and backward differences of the inverse Eqs. 53, 54, and 55.

Finite Difference Designation	Matrix of Coefficients			Right Hand Side
FFF	1	$R\,(z_{ij+1k} - z_{ijk+1})$	$-R\,(y_{ij+1k} - y_{ijk+1})$	$x_{i+1jk} - R\,(y_{ij+1k}\, z_{ijk+1}) + R\,(z_{ij+1k}\, y_{ijk+1})$
	$-R\,(z_{ij+1k} - z_{ijk+1})$	1	$R\,(x_{ij+1k} - x_{ijk+1})$	$y_{i+1jk} - R\,(z_{ij+1k}\, x_{ijk+1}) + R\,(x_{ij+1k}\, z_{ijk+1})$
	$R\,(y_{ij+1k} - y_{ijk+1})$	$-R\,(x_{ij+1k} - x_{ijk+1})$	1	$z_{i+1jk} - R\,(x_{ij+1k}\, y_{ijk+1}) + R\,(y_{ij+1k}\, x_{ijk+1})$
FFB	1	$-R\,(z_{ij+1k} - z_{ijk-1})$	$R\,(y_{ij+1k} - y_{ijk-1})$	$x_{i+1jk} + R\,(y_{ij+1k}\, z_{ijk-1}) - R\,(z_{ij+1k}\, y_{ijk-1})$
	$R\,(z_{ij+1k} - z_{ijk-1})$	1	$-R\,(x_{ij+1k} - x_{ijk-1})$	$y_{i+1jk} + R\,(z_{ij+1k}\, x_{ijk-1}) - R\,(x_{ij+1k}\, z_{ijk-1})$
	$-R\,(y_{ij+1k} - y_{ijk-1})$	$R\,(x_{ij+1k} - x_{ijk-1})$	1	$z_{i+1jk} + R\,(x_{ij+1k}\, y_{ijk-1}) - R\,(y_{ij+1k}\, x_{ijk-1})$
FBF	1	$-R\,(z_{ij-1k} - z_{ijk+1})$	$R\,(y_{ij-1k} - x_{ijk+1})$	$x_{i+1jk} + R\,(y_{ij-1k}\, z_{ijk+1}) - R\,(z_{ij-1k}\, y_{ijk+1})$
	$R\,(z_{ij-1k} - z_{ijk+1})$	1	$-R\,(x_{ij-1k} - x_{ijk+1})$	$y_{i+1jk} + R\,(z_{ij-1k}\, x_{ijk+1}) - R\,(x_{ij-1k}\, z_{ijk+1})$
	$-R\,(y_{ij-1k} - y_{ijk+1})$	$R\,(x_{ij-1k} - x_{ijk+1})$	1	$z_{i+1jk} + R\,(x_{ij-1k}\, y_{ijk+1}) - R\,(y_{ij-1k}\, x_{ijk+1})$
FBB	1	$R\,(z_{ij-1k} - z_{ijk-1})$	$-R\,(y_{ij-1k} - y_{ijk-1})$	$x_{i+1jk} - R\,(y_{ij-1k}\, z_{ijk-1}) + R\,(z_{ij-1k}\, y_{ijk-1})$
	$-R\,(z_{ij-1k} - z_{ijk-1})$	1	$R\,(x_{ij-1k} - x_{ijk-1})$	$y_{i+1jk} - R\,(z_{ij-1k}\, x_{ijk-1}) + R\,(x_{ij-1k}\, z_{ijk-1})$
	$R\,(y_{ij-1k} - y_{ijk-1})$	$-R\,(x_{ij-1k} - x_{ijk-1})$	1	$z_{i+1jk} - R\,(x_{ij-1k}\, y_{ijk-1}) + R\,(y_{ij-1k}\, x_{ijk-1})$
BFF	1	$-R\,(z_{ij+1k} - z_{ijk+1})$	$R\,(y_{ij+1k} - y_{ijk+1})$	$x_{i-1jk} + R\,(y_{ij+1k}\, z_{ijk+1}) - R\,(z_{ij+1k}\, y_{ijk+1})$
	$R\,(z_{ij+1k} - z_{ijk+1})$	1	$-R\,(x_{ij+1k} - y_{ijk+1})$	$y_{i-1jk} + R\,(z_{ij+1k}\, x_{ijk+1}) - R\,(x_{ij+1k}\, z_{ijk+1})$
	$-R\,(y_{ij+1k} - y_{ijk+1})$	$R\,(x_{ij+1k} - x_{ijk+1})$	1	$z_{i-1jk} + R\,(x_{ij+1k}\, y_{ijk+1}) - R\,(y_{ij+1k}\, x_{ijk+1})$
BFB	1	$R\,(z_{ij+1k} - z_{ijk-1})$	$-R\,(y_{ij+1k} - y_{ijk-1})$	$x_{i-1jk} - R\,(y_{ij+1k}\, z_{ijk-1}) + R\,(z_{ij+1k}\, y_{ijk-1})$
	$-R\,(z_{ij+1k} - z_{ijk-1})$	1	$R\,(x_{ij+1k} - x_{ijk-1})$	$y_{i-1jk} - R\,(z_{ij+1k}\, x_{ijk-1}) + R\,(x_{ij+1k}\, z_{ijk-1})$
	$R\,(y_{ij+1k} - y_{ijk-1})$	$-R\,(x_{ij+1k} - x_{ijk-1})$	1	$z_{il-jk} - R\,(x_{ij+1k}\, y_{ijk-1}) + R\,(y_{ij+1k}\, x_{ijk-1})$
BBF	1	$R\,(z_{ij-1k} - z_{ijk+1})$	$-R\,(y_{ij-1k} - y_{ijk+1})$	$x_{i-1jk} - R\,(y_{ij-1k}\, z_{ijk+1}) + R\,(z_{ij-1k}\, y_{ijk+1})$
	$-R\,(z_{ij-1k} - z_{ijk+1})$	1	$R\,(x_{ij-1k} - x_{ijk+1})$	$y_{i-1jk} - R\,(z_{ij-1k}\, x_{ijk+1}) + R\,(x_{ij-1k}\, z_{ijk+1})$
	$R\,(y_{ij-1k} - y_{ijk+1})$	$-R\,(x_{ij-1k} - x_{ijk+1})$	1	$z_{i-1jk} - R\,(x_{ij-1k}\, y_{ijk+1}) + R\,(y_{ij-1k}\, x_{ijk+1})$
BBB	1	$-R\,(z_{ij-1k} - z_{ijk-1})$	$R\,(y_{ij-1k} - y_{ijk-1})$	$x_{i-1jk} + R\,(y_{ij-1k}\, z_{ijk-1}) - R\,(z_{ij-1k}\, y_{ijk-1})$
	$R\,(z_{ij-1k} - z_{ijk-1})$	1	$-R\,(x_{ij-1k} - x_{ijk-1})$	$y_{i-1jk} + R\,(z_{ij-1k}\, x_{ijk-1}) - R\,(x_{ij-1k}\, z_{ijk-1})$
	$-R\,(y_{ij-1k} - y_{ijk-1})$	$R\,(x_{ij-1k} - x_{ijk-1})$	1	$z_{i-1jk} + R\,(x_{ij-1k}\, y_{ijk-1}) - R\,(y_{ij-1k}\, x_{ijk-1})$

The modified Gauss-Seidel method computes all eight of these differences, and the values of x_{ijk}, y_{ijk}, and z_{ijk} temporarily assigned to that grid point are determined by weighting these eight values according to the distance the grid point (ijk) is from the boundaries of the flow region. Thus, eight weighting factors are determined for each grid point. The weighting factors are equated to appropriate triple products of the following six integer quantities:

$$IF = I \quad \ldots\ldots\ldots\ldots\ldots\ldots (79)$$

$$IB = NP - I + 1 \quad \ldots\ldots\ldots\ldots\ldots\ldots (80)$$

$$JF = J \quad \ldots\ldots\ldots\ldots\ldots\ldots (81)$$

$$JB = NS - J + 1 \quad \ldots\ldots\ldots\ldots\ldots\ldots (82)$$

$$KF = K \quad \ldots\ldots\ldots\ldots\ldots\ldots (83)$$

$$KB = NSS - K + 1 \quad \ldots\ldots\ldots\ldots\ldots\ldots (84)$$

The first letter of these quantities denotes the ϕ, ψ, or ψ^* coordinate, respectively, and the second letter of the factor denotes forward or backward differences. The eight weighting factors are

$$F1 = (IF)\,(JF)\,(KF) \quad \ldots\ldots\ldots\ldots\ldots\ldots (85)$$

$$F2 = (IF)\,(JF)\,(KB) \quad \ldots\ldots\ldots\ldots\ldots\ldots (86)$$

$$F3 = (IF)\,(JB)\,(KF) \quad \ldots\ldots\ldots\ldots\ldots\ldots (87)$$

$$F4 = (IF)\,(JB)\,(KB) \quad \ldots\ldots\ldots\ldots\ldots\ldots (88)$$

$$F5 = (IB)\,(JF)\,(KF) \quad \ldots\ldots\ldots\ldots\ldots\ldots (89)$$

$$F6 = (IB)\,(JF)\,(KB) \quad \ldots\ldots\ldots\ldots\ldots\ldots (90)$$

$$F7 = (IB)\,(JB)\,(KF) \quad \ldots\ldots\ldots\ldots\ldots\ldots (91)$$

$$F8 = (IB)\,(JB)\,(KB) \quad \ldots\ldots\ldots\ldots\ldots\ldots (92)$$

The values of x, y, and z at each grid point are determined by

$$x_{ijk} = (x_1\,F1 + x_2\,F2 + x_3\,F3 + x_4\,F4 + x_5\,F5 + x_6\,F6 + x_7\,F7 + x_8\,F8)/T \quad \ldots\ldots\ldots\ldots\ldots\ldots (93)$$

$$y_{ijk} = (y_1\,F1 + y_2\,F2 + y_3\,F3 + y_4\,F4 + y_5\,F5 + y_6\,F6 + y_7\,F7 + y_8\,F8)/T \quad \ldots\ldots\ldots\ldots\ldots\ldots (94)$$

$$z_{ijk} = (z_1\,F1 + z_2\,F2 + z3\,F_3 + z_4\,F_4 + z_5\,F5 + z_6\,F6 + z_7\,F7 + z_8\,F8)/T \quad \ldots\ldots\ldots\ldots\ldots\ldots (95)$$

in which $x_1, x_2, x_3, \ldots, x_8, y_1, y_2, \ldots, y_8, z_1, z_2, \ldots, z_8$ are the solutions of the eight possible equations denoted by Eq. 78, and T is the sum of F1, F2, F3, ..., F8. As an example, the unknown values at grid point i=2, j=2, and k=2 in a Dirichlet boundary value problem will have larger weighting factors associated with the BBB than FFF differences, because backward differences use preceding information, which are correct values from the boundaries, while forward differences use succeeding information, which are interior variables whose values must eventually be determined from the boundary values to satisfy the partial differential equations.

The performance of the modified Gauss-Seidel method was studied initially by introducing errors into the interior grid points of a uniform flow, Dirichlet boundary value problems and observing if each subsequent iteration gave a solution that better approximated the uniform flow values. The results of the method were satisfactory, with reasonably rapid convergence occurring. An indication of rates of convergence that can be achieved is given later in discussing the particular solutions which have been obtained.

BOUNDARY CONDITIONS

The boundary condition equations for some of the boundaries can be obtained by simplifying the basic inverse equations by noting that some of the dependent variables and derivatives are known. On the other hand, the free surface boundary and the body boundaries present special problems, and consequently these boundary conditions will be discussed in the next section. The boundary conditions for boundaries 1, 2, 3, and 4 of Figure 1 will be described in this section, with boundary 3 considered as a confining boundary. On these boundaries, derivatives with respect to one of the independent variables are known; consequently, only two of the three inverse equations are required to solve for the two unknown dependent variables (see Table 2).

Table 2. Boundary conditions along a rectangular conduit. (See Figure 2.)

Side	Zero derivatives and constant values	Equations used to solve for unknows	Finite difference combinations used
1	$y = 0$ $\partial x/\partial\psi = 0$ $\partial z/\partial\psi = 0$	$\frac{\partial x}{\partial\phi} = \frac{\partial y}{\partial\psi}\frac{\partial z}{\partial\psi^*} R$ $\frac{\partial z}{\partial\phi} = -\frac{\partial y}{\partial\psi}\frac{\partial x}{\partial\psi^*} R$	FFF FFB BFF BFB
2	$z = \text{constant} = 1$ $\frac{\partial y}{\partial\psi^*} = 0$ $\frac{\partial x}{\partial\psi^*} = 0$	$\frac{\partial x}{\partial\phi} = \frac{\partial y}{\partial\psi}\frac{\partial z}{\partial\psi^*} R$ $\frac{\partial y}{\partial\phi} = -\frac{\partial x}{\partial\psi}\frac{\partial z}{\partial\psi^*} R$	FFB FBB BFB BBB
3	$y = \text{constant} = \frac{D}{W}$ $\frac{\partial x}{\partial\psi} = 0$ $\frac{\partial z}{\partial\psi} = 0$	$\frac{\partial x}{\partial\phi} = \frac{\partial y}{\partial\psi}\frac{\partial z}{\partial\psi^*} R$ $\frac{\partial z}{\partial\phi} = -\frac{\partial y}{\partial\psi}\frac{\partial x}{\partial\psi^*} R$	FBF FBB BBF BBB
4	$z = 0$ $\frac{\partial y}{\partial\psi^*} = 0$ $\frac{\partial x}{\partial\psi^*} = 0$	$\frac{\partial x}{\partial\phi} = \frac{\partial y}{\partial\psi}\frac{\partial z}{\partial\psi^*} R$ $\frac{\partial y}{\partial\phi} = -\frac{\partial x}{\partial\psi}\frac{\partial z}{\partial\psi^*} R$	FFF FBF BFF BBF
5	$x = 0$	$y = \frac{j}{NS}\frac{D}{W}$ $z = \frac{k}{NSS}$	None
6	$x = \text{constant} = x_f$	$y = \frac{j}{NS}\frac{D}{W}$ $z = \frac{k}{NSS}$	None

Uniform flow is assumed to exist through sides 5 and 6, so the values y and z are known on these boundary planes. Furthermore, on side 5, x is constant and can be assigned the value zero. On side 6, x is constant, but of unknown value x_f. Only if uniform flow exists throughout the flow field will x_f equal unity by virtue of the nondimensionalization process regardless of the number of equipotential surfaces assigned. When nonuniform flow exists in the region, x_f must be determined as explained subsequently. To illustrate why $x_f = 1$ for uniform flow, note that the derivatives $\partial y/\partial\psi$ and $\partial z/\partial\psi^*$ are constant and independent of the number of equipotential planes. Consequently, along boundaries 1 and 3, Eq. 53 reduces to

$$C\frac{\partial x}{\partial\phi} = \frac{NP1}{(NS1)(NSS1)}\frac{\partial x}{\partial\phi} = \frac{\partial y}{\partial\psi}\frac{\partial z}{\partial\psi^*} = K \quad \ldots(96)$$

or

$$NP1\ \frac{\partial x}{\partial\phi} = K' \quad \ldots(97)$$

in which K and K' are constants, because NS1 and NSS1 can remain constant as NP1 is assigned any desired value. Substituting differences in Eq. 97 produces

$$NP1\ \frac{\Delta x}{\Delta\phi} = K' \quad \ldots(98)$$

but $\Delta\phi = 1$ by choice, so (NP1) x (Δx) = K' ; if NP1 is increased, Δx must decrease proportionately to retain a constant product. The result is that x_f equals unity for any assigned value of NP1 when uniform flow exists.

When nonuniform flow exists in the flow field, $\partial y/\partial\psi$ and $\partial z/\partial\psi^*$ vary from grid point to grid point, so x_f must be evaluated by integrating Eq. 96 along ψ^* constant planes as denoted by the following equation:

$$x_{i+1jk} = x_{ijk} + R\int_i^{i+1}\left[\left(\frac{\partial y}{\partial\psi}\frac{\partial z}{\partial\psi^*}\right)_{ijk}\right]d\phi \quad \ldots(99)$$

i = 1, 2, ..., NP1; j = constant; k = constant

At the beginning of the solution process x_f will be different from each path of integration. As the modified Gauss-Seidel iteration approaches the final solution, however, the value of x_f obtained from each path should approach the same value. Until this occurs the average of the individual x_f is taken as the constant for side 6.

The boundary conditions given in Table 2 are among the simplest possible for three-dimensional flows. Boundary conditions for physical spaces where the boundaries are not planar and are not normal to one another would have no variable constant throughout its plane in the inverse space.

FREE SURFACE

The Bernoulli equation is valid throughout the flow field and can be written as

$$\frac{V^2}{2g} + Y = \frac{u^2+v^2+w^2}{2g} + Y = H \quad \ldots\ldots \quad (100)$$

on the free surface with the pressure assigned a value of zero. Substituting Eqs. 12, 13, and 14 for u, v, and w, and noting that

$$J = (u^2+v^2+w^2) \quad \ldots\ldots\ldots\ldots \quad (101)$$

produces

$$\left(\frac{\partial X}{\partial \Phi}\right)^2 + \left(\frac{\partial Y}{\partial \Phi}\right)^2 + \left(\frac{\partial Z}{\partial \Phi}\right)^2 = \frac{1}{2g\,(H-Y)} \quad \ldots\ldots \quad (102)$$

The dimensionless form of Eq. 102 is

$$\left(\frac{\partial x}{\partial \phi}\right)^2 + \left(\frac{\partial y}{\partial \phi}\right)^2 + \left(\frac{\partial z}{\partial \phi}\right)^2 = \frac{COG4}{(h-y)} \quad \ldots\ldots \quad (103)$$

in which

$$COG4 = \frac{Q^2}{(NP1^2)\,(W^5)\,(2g)} \quad \ldots\ldots\ldots \quad (104)$$

and

$$h = H/W \quad \ldots\ldots\ldots\ldots\ldots \quad (105)$$

Equation 103 can be integrated to obtain the x variables at each grid point on the free surface by using the following equation:

$$x_{i+1jk} = x_{ijk} + \int_i^{i+1} \sqrt{\left[\frac{COG4}{h-y} - \left(\frac{\partial y}{\partial \phi}\right)^2 - \left(\frac{\partial z}{\partial \phi}\right)^2\right]}\, d\phi \quad (106)$$

The magnitudes of $\partial y/\partial \phi$ and $\partial z/\partial \phi$ are generally small in comparison to the magnitude of $\partial x/\partial \phi$, so any error in evaluating the derivatives within the square root sign causes a small percentage error in evaluating x. For this reason, $\partial y/\partial \phi$ and $\partial z/\partial \phi$ are considered known during the integration process, which is continually repeated anyway until the correct solutions to all unknowns x, y, and z are obtained.

If poor initial values are used, the argument within the square root sign can become negative, particularly in the region where $\partial y/\partial \phi$ and $\partial z/\partial \phi$ are large. Should this occur during the execution of the computer program, the argument is set equal to zero.

Equation 53 can be rearranged and integrated to evaluate z at each free surface grid point, as follows:

$$z_{ijk+1} = z_{ijk} + \int_k^{k+1} \left[\frac{C\frac{\partial x}{\partial \phi} + \frac{\partial z}{\partial \psi}\frac{\partial y}{\partial \psi^*}}{\frac{\partial y}{\partial \psi}}\right] d\psi^* \quad . \quad (107)$$

The solution for y on the free surface is more difficult to obtain since it cannot be solved for explicitly from the dimensionless Bernoulli Eq. 103 under the assumption that x and z are known. Jeppson (15) examined the function

$$F_1 = \left(\frac{\partial y}{\partial \psi}\frac{\partial z}{\partial \psi^*} - \frac{\partial z}{\partial \psi}\frac{\partial y}{\partial \psi^*}\right)^2 + C^2\left(\frac{\partial y}{\partial \phi}\right)^2 + \left(\frac{\partial x}{\partial \psi}\frac{\partial y}{\partial \psi^*} - \frac{\partial y}{\partial \psi}\frac{\partial x}{\partial \psi^*}\right)^2 - \frac{CGQ}{h-y} = 0 \quad \ldots\ldots \quad (108)$$

in which

$$CGQ = \frac{Q^2}{(NS1)^2\,(NSS1)^2\,(W)^5\,(2g)} \quad \ldots\ldots \quad (109)$$

in solving for y on the free surface. Graphs of the function F_1 versus $y_{i,NS,k}$, with errors existing in surrounding grid points, as indicated, are shown in Figure 6. Four roots of F_1 are seen to exist in Figure 7, but the root to the right of y = h can be discarded since the depth cannot exceed the total head, and the root occurring at approximately y = 0.88 can be eliminated by examination of the problem being solved. However, the two zeroes of the function that occur near y = 1.0 are both candidates for the correct root. Jeppson concluded that the positively sloped root was always the correct one, but he used a slightly different definition of the dimensionless independent variables and did not make the dependent variables nondimensional. This investigation supported the

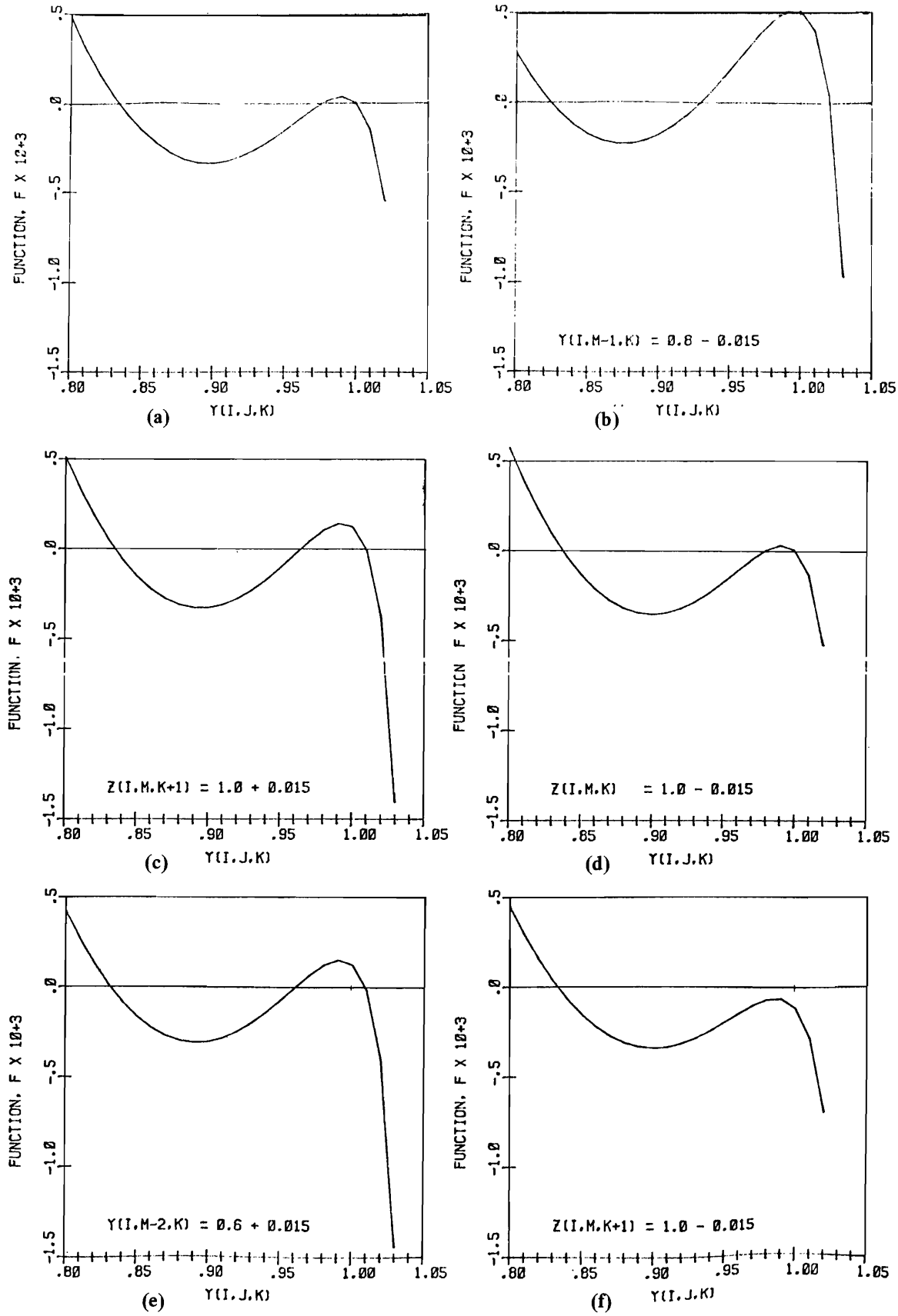

Figure 6. Function defined by Eq. 108 versus y_{ijk} with errors in surrounding points.

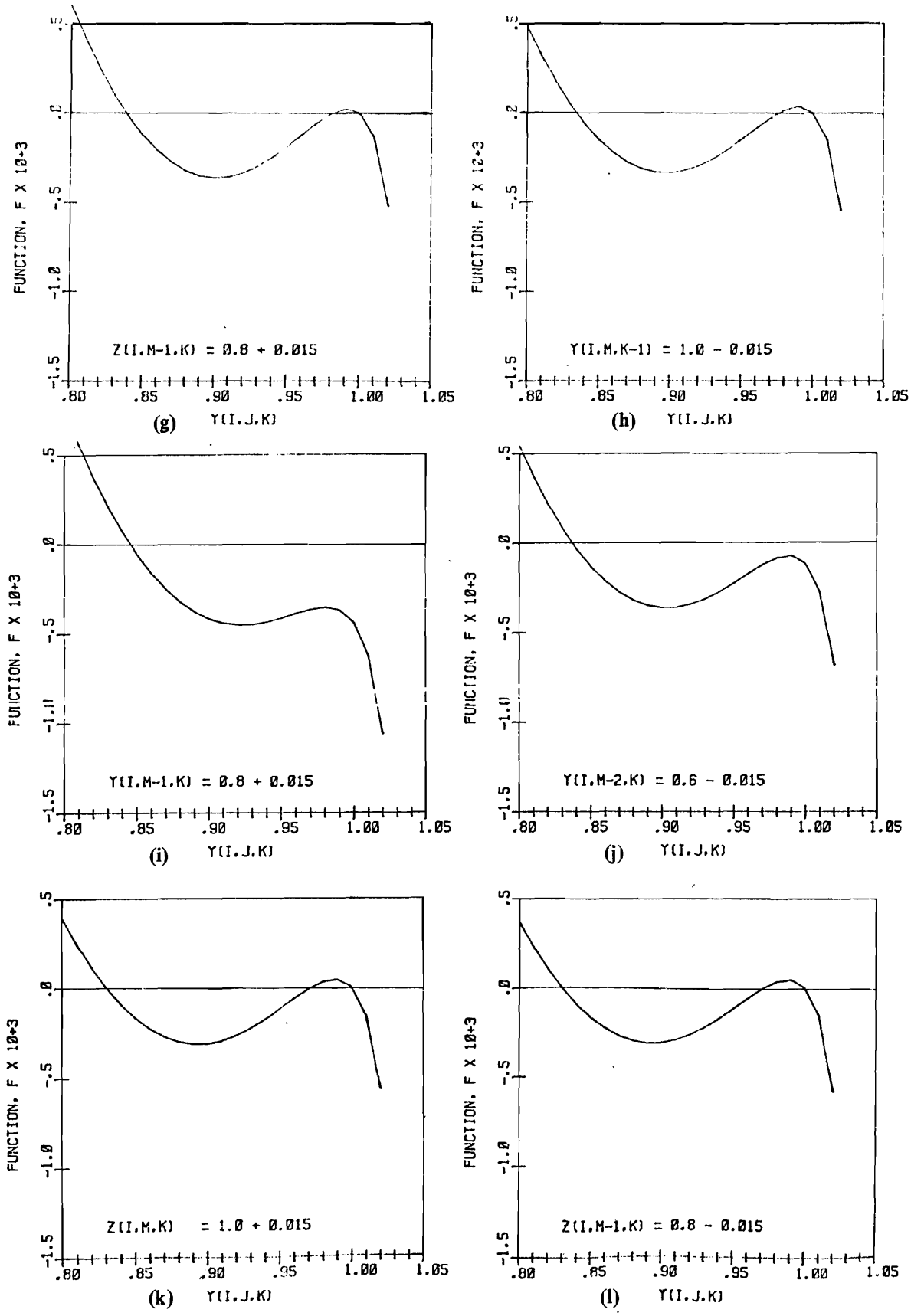

Figure 6. Continued.

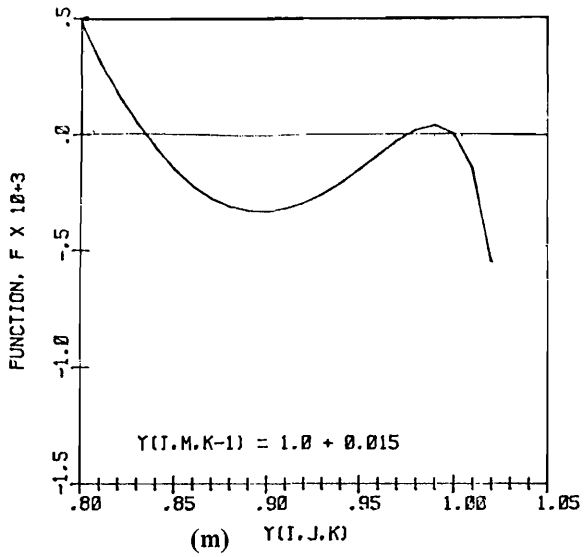

(m)

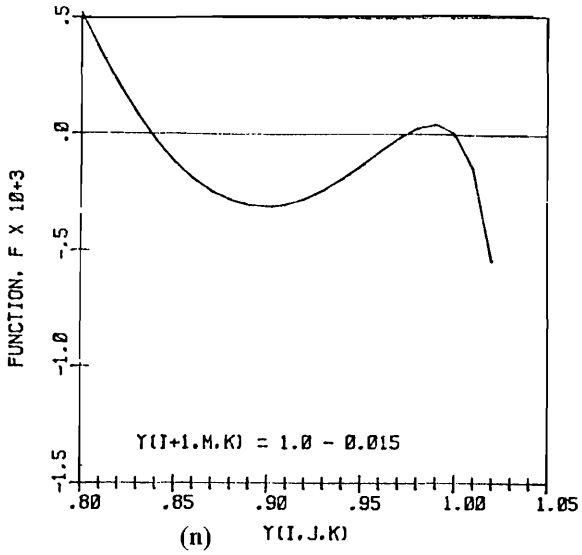

(n)

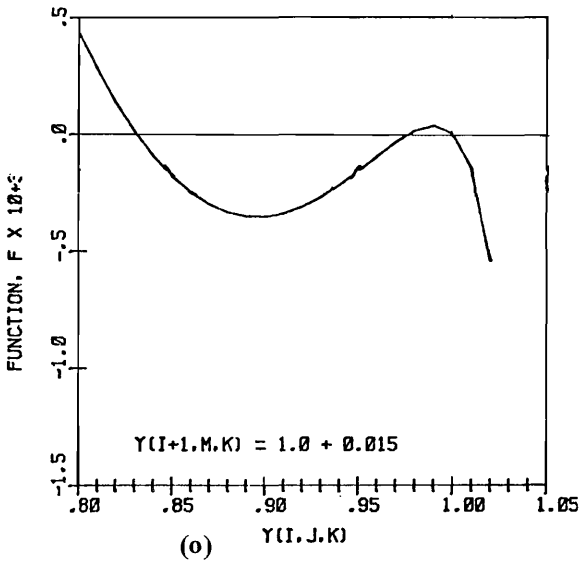

(o)

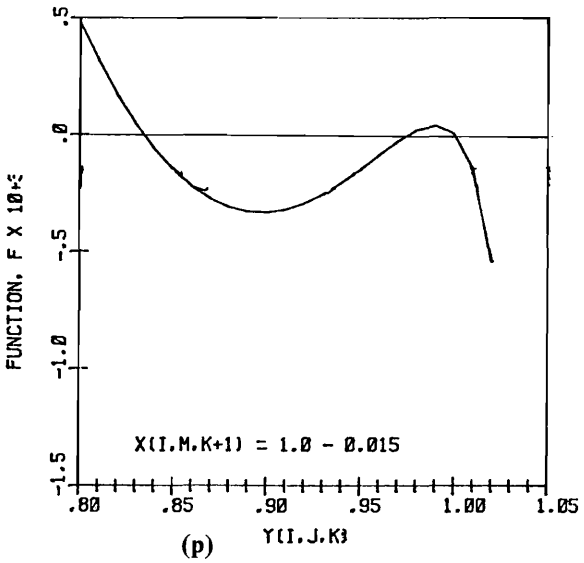

(p)

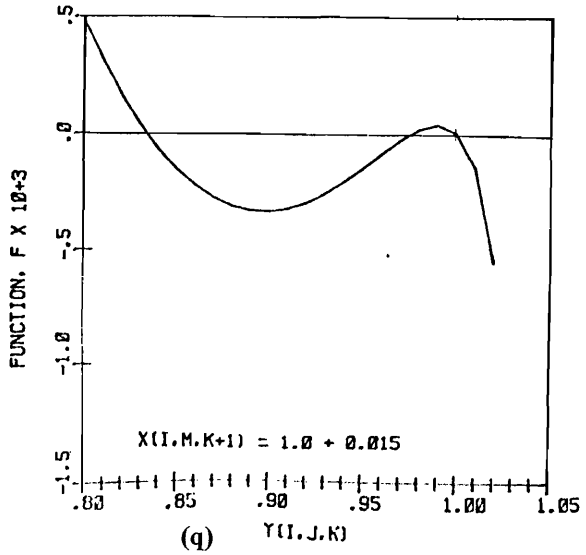

(q)

Figure 6. Continued.

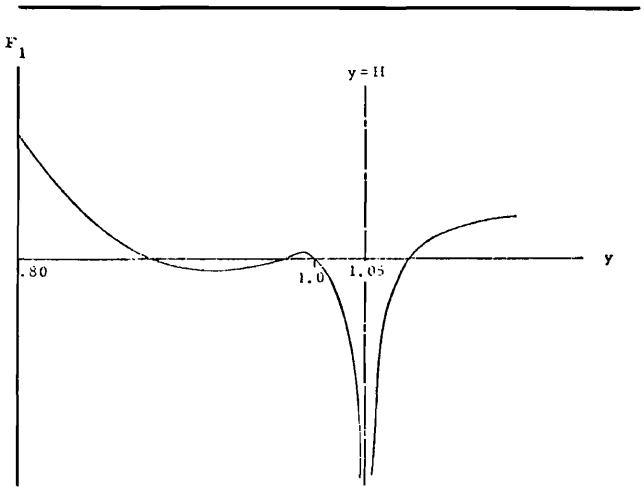

Figure 7. Graph of F_1 vs. y showing the roots of the equation that exist in obtaining a solution for y on the free surface.

negatively sloped root as the correct one in all cases. In any event, the two roots are not far apart if they exist at all. Errors in certain of the surrounding grid points cause no roots to exist in the range of y values where a correct solution could exist. The range of possible solutions will be referred to as the feasible region. The bounds for this egion must be determined by judgment and insight.

If two roots occurred in the feasible region (see Figure 6-a), the methods of False-position and Newton-Raphson (11) were used to obtain the solution. If no roots were present in the feasible region (see Figure 6-f), the Fibonacci search method (25) was used to obtain the maximum value the function F_1 reached, and this maximum value was used to approximate the correct solution.

A more satisfactory approach was to rewrite Eq. 103, after substituting for $\partial z/\partial \phi$, as

$$F_2 = C^2 \left[\left(\frac{\partial x}{\partial \phi}\right)^2 + \left(\frac{\partial y}{\partial \phi}\right)^2\right] + \left(\frac{\partial x}{\partial \psi}\frac{\partial y}{\partial \psi^*} - \frac{\partial y}{\partial \psi}\frac{\partial x}{\partial \psi^*}\right)^2 - \frac{CGQ}{h-y} = 0 \quad (110)$$

Graphs of F_2 versus $y_{i,NS,k}$, with errors existing in surrounding grid points are shown in Figure 8. Only one root occurs in the feasible region, even when errors exist in surrounding grid points, and this root is obtained using the False-position method. If the root is not located in a specified number of iterations during execution of computer program, the y variable is equated to the average of the four surrounding free surface y values.

The function defined as

$$F_3 = \left[\left(\frac{\partial x}{\partial \phi}\right)^2 + \left(\frac{\partial y}{\partial \phi}\right)^2 + \left(\frac{\partial z}{\partial \phi}\right)^2\right] - \frac{COG4}{h-y} = 0 \quad (111)$$

is similar to F_2 (see Figure 9). However, the variable z is eliminated from Eq. 110, so it is used in preference to Eq. 111.

At the intersection of the free surface boundary with sides 2 and 4 of Figure 1b, the x and y variables need to be determined subject to the boundary conditions from both the free surface and the sides. A preliminary attempt at combining the side and free surface boundary conditions and incorporating them into the inverse equations, so x and y could be determined, indicated that the variables were allowed to "float" too freely to obtain a satisfactory solution for the other free surface grid points by using the values established from the intersecting boundaries. The x and y values along the two lines of intersection are determined, in part, from the values on the free surface, and the free surface values are influenced by the values along the lines of intersection; the interdependence between the lines of intersection and the free surface creates a nonconvergent process when the variables are evaluated in this manner.

An alternate approach, which proved to be more satisfactory, was to use a third degree polynomial involving other free surface y values along a ϕ constant plane to extrapolate suitable y values at the two lines of intersection between the free surface and the side boundaries. The coefficients of the polynomials were determined by multiple regression (5), using the free surface y values from k=2 to k=NSS1 along a ϕ constant plane as the known points.

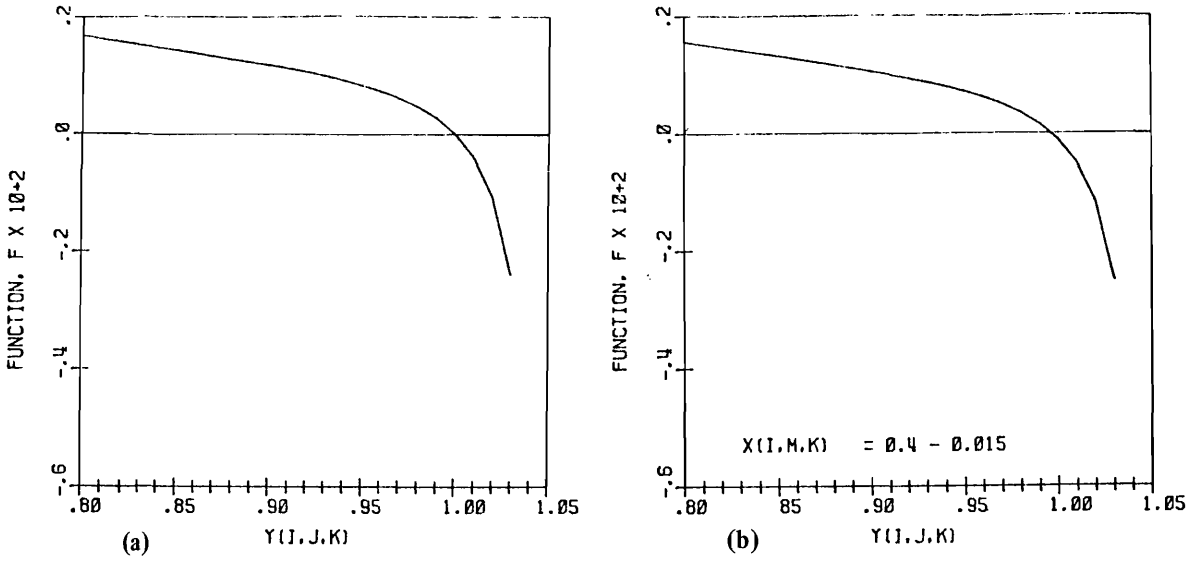

Figure 8. Function defined by Eq. 110 versus y_{ijk} with errors in surrounding points.

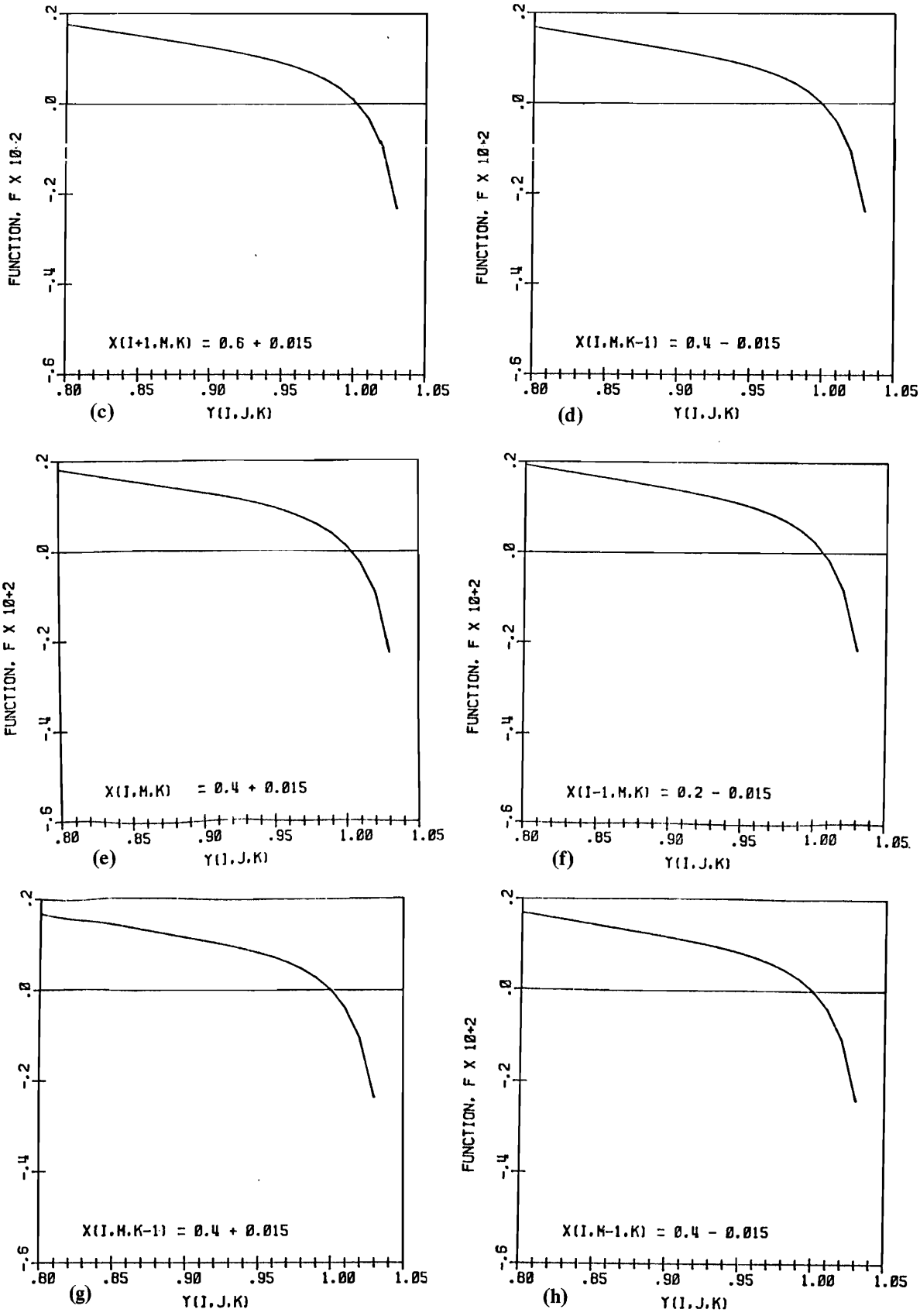

Figure 8. Continued.

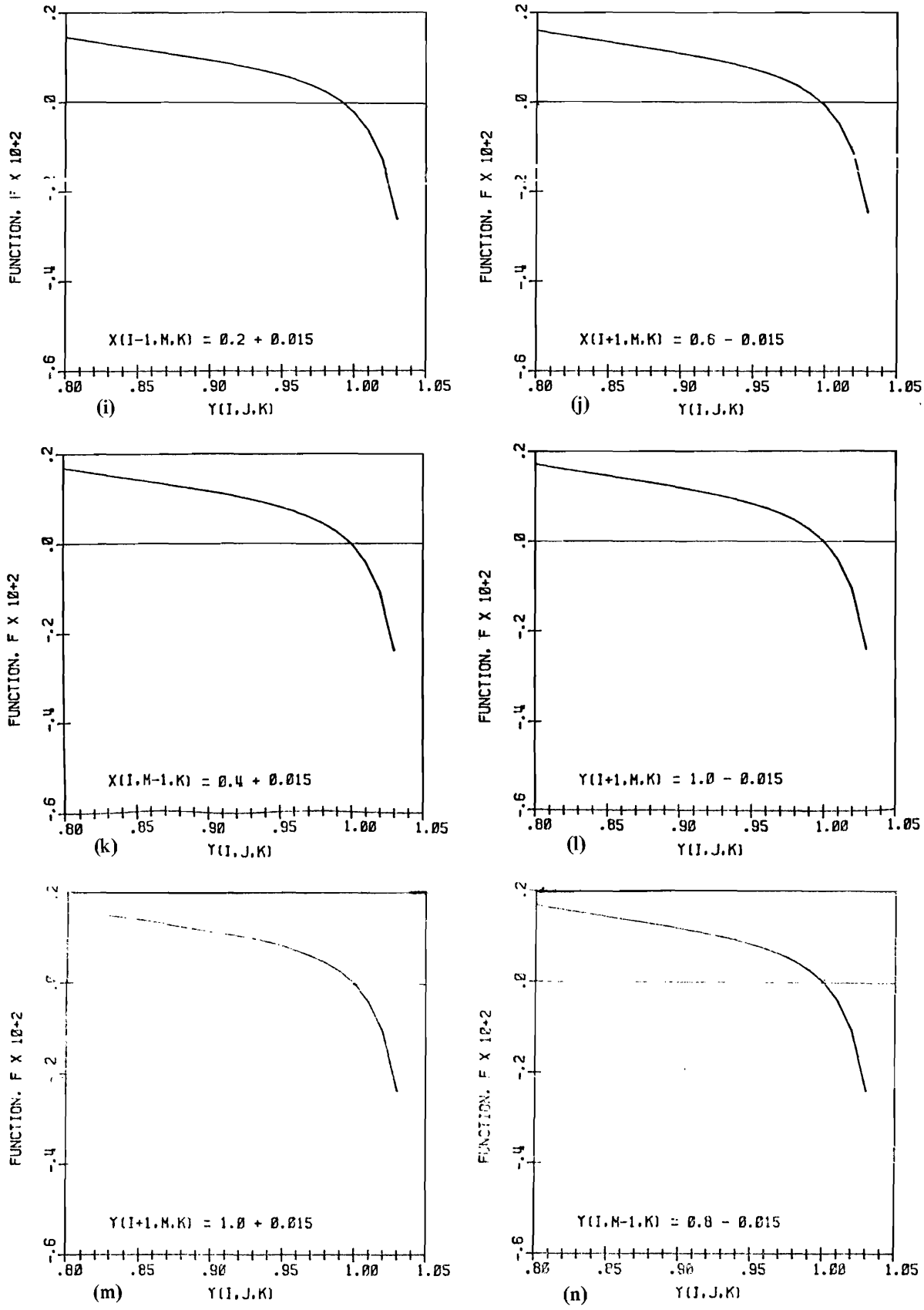

Figure 8. Continued.

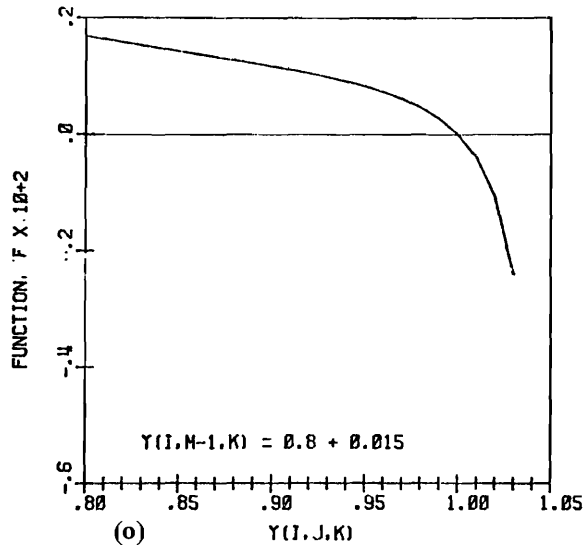

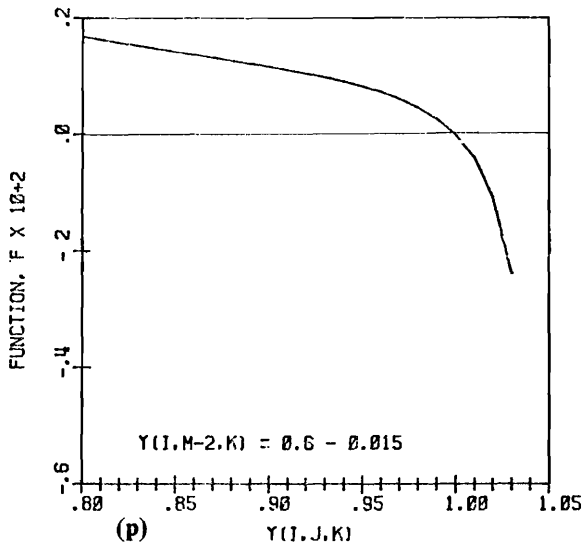

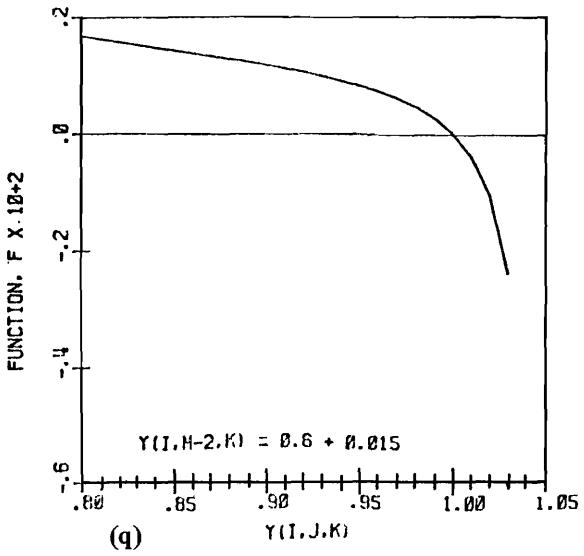

Figure 8. Continued.

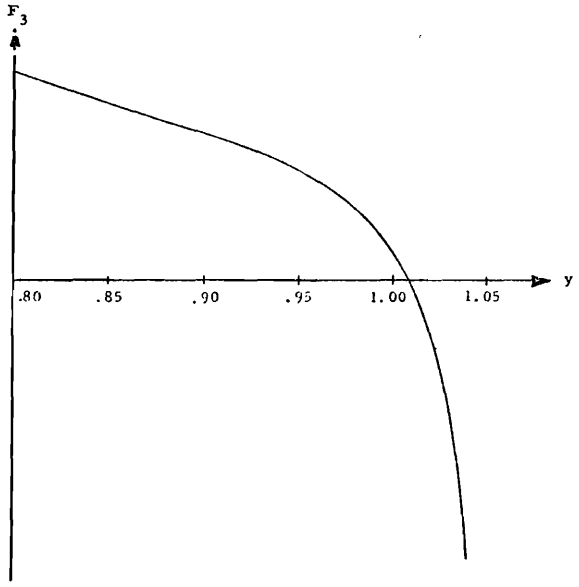

Figure 9. Graph of F_3 vs. y showing the single root that exists in obtaining y on the free surface.

FLOW AROUND A BODY

Since this study was exploratory in the development of methods for solving three-dimensional, free surface, potential flow problems using the inverse formulation described previously, the first problems examined were made simple intentionally. After satisfactory performance of the method was achieved in solving the simplified problems, additional features were added, one at a time, increasing the complexity of the problem and requiring greater capability of the solution method. In accordance with this philosophy, the first problem examined consisted of a body placed within the flow in a rectangular duct. This problem was used to develop and investigate appropriate means for specifying a body within the flow in the inverse formulation and to develop schemes for obtaining a solution thereof. After being satisfied with the performance of the method for describing the flow around the body with specified exterior boundaries, the solution capability was expanded by removing the top of the duct and replacing it with the free surface condition in a vertical gravitational field. These problems will be described in this sequence in this and the following sections.

The ψ and ψ^* constant surfaces separate at the stagnation points of flow around an object placed entirely within the flow field. These surfaces, which are separated around the body in the physical space, are collapsed onto a divided line in the inverse space. Thus all paths from the front to the rear of the body are along the same line in the inverse space. Four separate paths have been used to define the body as shown in Figures 10 and 11. In the computer program, separate two-dimensional arrays (with the second subscript used to denote the path), have been added to store the values of the dependent variables along these separate paths. Thus XB(I,NUM), YB(I,NUM), and ZB(I,NUM) replace the values of x(I,MB,NB), y(I,MB,NB), and z(I,MB,NB), in which I takes on the values LB (corresponding to the upstream stagnation point) to LN (corresponding to the downstream stagnation point), MB and NB correspond to ψ and ψ^* planes, respectively, which define the position of the body, and NUM corresponds to the path followed, as illustrated in Figure 10a. The values of the dependent variables x, y, and z along each separate path help determine the shape and position of the body in the flow field, and each such value must either be specified or computed. Since x, y, and z are related, only two can be specified and the third must be computed to satisfy the differential equations. The arrays YB and ZB are specified as deviations from y and z at the upstream stagnation point for each NUM path along the body. To satisfy Eqs. 53 through 55, XB must be calculated at each equipotential surface along each NUM path by using the following equation:

$$XB(I+1,NUM) = XB(I,NUM) + 13/24(F_I + F_{I+1}) - 1/24(F_{I+2} + F_{I-1}) \quad (112)$$

in which

$$F_i = R\left(\frac{\partial y}{\partial \psi}\frac{\partial z}{\partial \psi^*} - \frac{\partial z}{\partial \psi}\frac{\partial y}{\partial \psi^*}\right)_i, \quad i = I-1 \text{ to } I+2, \quad I = LB \text{ to } LN-1 \quad (113)$$

The values XB(LN,NUM), which occur at the rear stagnation point, must be equal regardless of the NUM path followed. However, differences in the final x values on the body will exist during the solution process because the variables involved in the derivatives $\partial y/\partial \psi$, $\partial z/\partial \psi^*$, $\partial z/\partial \psi$, and $\partial y/\partial \psi^*$ are also being adjusted, and consequently they are not free from error. The difference between each value in XB(LN,NUM) for NUM = 1,2, ... 4 and the value x(LN,MB,NB), which is obtained by integrating Eq. 53 in the negative ϕ direction from the NP to the LN equipotential surface, is distributed linearly back along each NUM path to adjust the values XB(I,NUM).

Second order forward and backward differences are used to evaluate the derivatives $\partial y/\partial \psi$, $\partial z/\partial \psi^*$, $\partial z/\partial \psi$, and $\partial y/\partial \psi^*$ along the body. A value on the body is used in conjunction with two values adjacent to the divided line representing the body in the inverse space to evaluate these derivatives. The body value that is closest in the physical space to the adjacent values used to evaluate the derivatives is used. For example, referring to Figure 11a, if a forward difference is used to evaluate a derivative with respect to ψ^*, NUM path 4 is used to supply the body value, because it has more influence in determining the correct value of a variable at the (ψ, ψ^*+1) grid point than the body value from any other path.

The velocity at the stagnation points is zero, so these points are singularities. The sum of the squares of the derivatives $\partial x/\partial \phi$, $\partial y/\partial \phi$, and $\partial z/\partial \phi$ must then be infinite at the singularities, since

$$\left(\frac{\partial x}{\partial \phi}\right)^2 + \left(\frac{\partial y}{\partial \phi}\right)^2 + \left(\frac{\partial z}{\partial \phi}\right)^2 = \frac{\text{FACTOR}}{V^2} = \frac{\text{FACTOR}}{0} = \infty \quad (114)$$

in which FACTOR is a positive quantity. Finite differences do not yield infinite values for these derivatives at the stagnation points. Therefore, the error in the finite difference solution is greatest in regions around the stagnation points. In obtaining finite difference solutions to two-dimensional problems, analytic solutions have been patched in around the singularities. However, for three-dimensional problems with gravity, analytic solutions are not available. Hence, adjustments to the dependent variables near the singularities must be based on judgment, if indeed adjustments are made.

The exact shape a body assumes during the solution procedure cannot be predicted initially, because the variable x along the body must be determined as part of the solution. However, desired shapes can be obtained by trial and error by adjusting the variables y and z along the body.

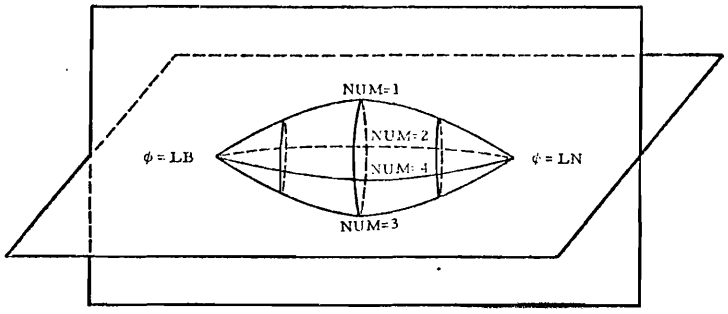

(a) Physical Space

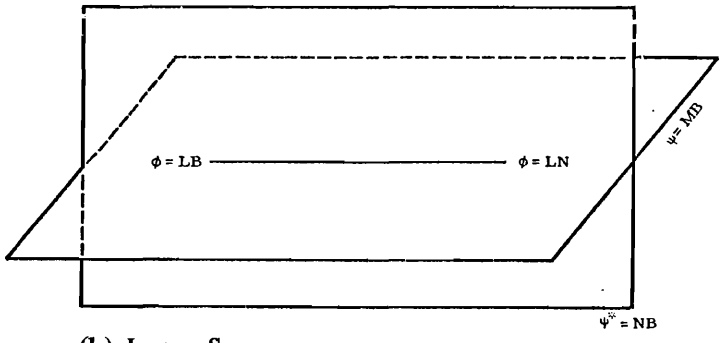

(b) Inverse Space

Figure 10. Illustration of a body in the physical space collapsed onto a divided line in the inverse space.

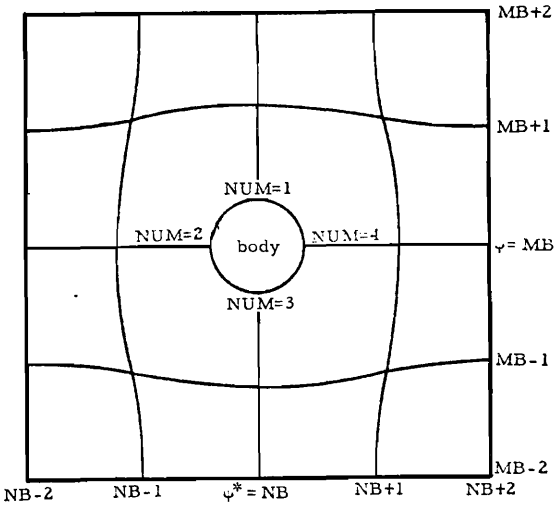

(a) Physical Space

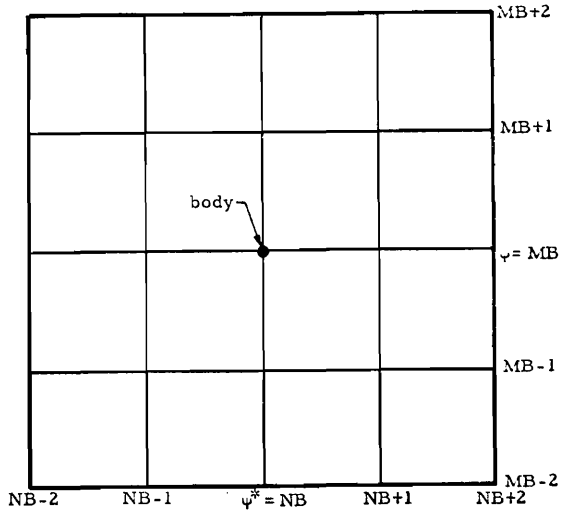

(b) Inverse Space

Figure 11. Cross section of a three-dimensional body at a constant equipotential surface in (a) the physical space, showing the paths that can be followed along the body from the upstream to the downstream stagnation point; (b) in the inverse space, showing the body cross section collapsed onto a point.

CAVITY FORMATION BEHIND A BODY

In studying cavities (2,9,10), the following dimensionless cavitation number is commonly used:

$$\sigma = \frac{p_o - p_c}{\frac{1}{2}\rho V_o^2} \quad \ldots \ldots \ldots \ldots \ldots \quad (115)$$

in which p_c is the constant pressure inside the cavity, ρ is the fluid density, and V_o and p_o are the velocity and pressure at a reference point in the flow. A convenient reference point is the top surface upstream from the body where uniform flow exists and where the pressure is atmospheric if a free surface is present. The depth at this point will be denoted by Y_o ($y_o = Y_o/W$). The velocity along the cavity surface is related to σ, V_o, y_o, and to the dimensionless vertical distance from the channel bottom to the cavity surface y (y = Y/W) through the Bernoulli equation as follows:

$$V_c^2 = V_o^2(\sigma + 1) + 2g(W)(y_o - y) \quad \ldots \ldots \quad (116)$$

In the following paragraphs a method is described for obtaining finite difference solutions to problems in which a cavity forms downstream from a body. Comprehension of the method in principle is not difficult, but its implementation in a satisfactory computer solution requires considerable logic and generally 2 or 3 times as much storage. A workable computer program for solving cavity problems has not been developed at present.

In the inverse space, the cavity is collapsed onto an extension of the line defining the body in the flow (see Figures 2, 10, 11). The equipotential surface where the body ends can be specified as NCB. The end of the cavity will occur at a downstream point where the y-values from different paths along the cavity surface become equal. The number of the finite difference index i denoting the equipotential surface nearest this point will be denoted by LN. (The value LN is used to denote the final downstream finite difference index of the line in the inverse space that defines either a body or a body and cavity.) The correct value of LN must be determined as part of the solution. This determination of LN, which is closely associated with the cavity length as well as the determination of the cavity shape, might proceed by initially specifying the z-coordinate at each ϕ constant surface along the cavity for each NUM path by estimating the shape of the cavity for some estimated value of LN. (Initial values of x and y are also supplied as part of the flow field initialization.) The corresponding x- and y-coordinates can then be calculated as described.

The x-coordinates along the cavity for each NUM path can be determined by the following equation, which assumes y is known temporarily along the cavity surface:

$$x_{i+1jk} = x_{ijk} + \int_i^{i+1} \sqrt{\frac{COG5}{CK4 - 2g(W)(y)} - \left(\frac{\partial y}{\partial \phi}\right)^2 - \left(\frac{\partial z}{\partial \phi}\right)^2}\, d\phi \quad \ldots \quad (117)$$

in which j and k equal the index numbers assigned to the stream functions coincident with the cavity,

$$COG5 = \frac{Q^2}{(W^4)(NPl^2)} \quad \ldots \ldots \ldots \ldots \quad (118)$$

and

$$CK4 = V_o^2(\sigma + 1) + 2g(W)(y_o) \quad \ldots \ldots \quad (119)$$

The y-coordinates at each ϕ constant plane and along each NUM path on the cavity surface are adjusted to satisfy the following implicit equation by the same procedure described earlier for adjusting y on the free surface.

$$F_4 = \left(\frac{\partial x}{\partial \phi}\right)^2 + \left(\frac{\partial y}{\partial \phi}\right)^2 + \left(\frac{\partial z}{\partial \phi}\right)^2 - \frac{COG5}{GK4 - 2g(W)(y)} = 0 \quad \ldots \quad (120)$$

To simplify the procedure for developing a cavity solution, the body could be shaped and positioned symmetrically with respect to z.

If the YB(LN,NUM) values from paths NUM=1 and NUM=3 are equal within a specified tolerance limit, the value of LN requires no further adjustment for the present iteration. Periodically, after the interior variables have their values altered by the modified Gauss-Seidel method, the same procedure for computing x and y will be repeated. If YB(LN,1) is less than YB(LN,3), LN should be decreased by one; if the reverse is true, LN should be increased by one. Immediately after LN is decreased, the ZB(I,NUM) variables along each NUM path on the cavity surface should be adjusted by subtracting ZB(LN,NUM) times the ratio (I-NCB)/(LN-NCB), I=NCB+1,..., LN-1, from ZB(I,NUM).

If LN is increased, the values ZB(I,NUM) should be increased; for example,

$$ZB(I,NUM)_{t+1} = ZB(I,NUM)_t + DELTA\left(\frac{I - NCB}{LN - NCB}\right) \quad . \quad . \quad . \quad . \quad (121)$$

where DELTA is a specified amount of increase, such as ZB(NCB,NUM)/(LN-NCB), and I=NCB+1,..., LN-1. In making these adjustments of ZB(I,NUM), all values from separate NUM paths must be equal upon closing the cavity at the new LN.

The YB(I,NUM) variables from the previous iteration, where I=NCB+1, ..., LN-1, can then be adjusted by following a procedure similar to that used to adjust the ZB(I,NUM) variables. The XB(I,NUM) and YB(I,NUM) variables can then be determined again from Eqs. 117 and 120 as described previously. Then the entire process can be repeated iteratively until the cavity closes properly with the LN value used.

When the general direction of flow is horizontal and gravitational forces act vertically, the vertical coordinate of the point where the cavity closes cannot be determined except as a part of the solution. Hence, establishing the shape of the cavity and the location of the point of cavity closing will likely necessitate checking to insure that no condition of the flow is violated.

REFLECTIONS ON INVERSE METHODS

Before presenting several numerical solutions to problems of three-dimensional potential flows about bodies, the advantages of the methods described herein over the more conventional noninverse-finite difference methods will be enumerated, and also the limitations of the methods will be discussed.

Major advantages to use of the inverse formulation are:

1. Whenever a potential flow problem can be confined within the space contained between two equipotential surfaces, and four stream surfaces, two of which are orthogonal to the other two, then the region of the inverse space boundary-value problem is a parallelepiped (i.e. all boundaries are plane surfaces), regardless of how irregular or wavy the boundaries are in the physical space, or even if their position is unknown. What the inverse formulation accomplishes is that free surfaces (position unknown in physical space) and other irregular boundaries which are stream surfaces of the flow are transformed into planes. Consequently, potential flow problems whose boundaries are unknown in the physical space (i.e. a space boundary value problem with unknown boundary positions and shapes) is placed into a space in which the boundary value problem has all plane boundaries.
2. From non-Dirichlet boundary conditions, finite difference operators can be developed which supply values to the dependent variables (x,y, and z) in the same manner as the finite difference operators for interior grid points supply values of the dependent variables throughout the flow field.
3. The form of the solution is ideal in that the streamlines (i.e. intersection of orthogonal stream surfaces) and potential surfaces are given directly from the solution, from which other quantities of interest such as velocity, pressure and gradients thereof can readily be computed. If potential surfaces are desired from solutions in the physical space, they must be interpolated between the values at the grid points, and as far as the writers are aware no one has perfected methods for obtaining the stream surfaces for three-dimensional solutions to ϕ in the physical space even though the equations exist which relate stream surface functions to the potential function.
4. Once fully perfected, the methods can handle a diversity of free flow and cavity problems as well as design problems with only minor changes in the solution procedure.

These advantages are accompanied by:

1. The necessity of solving three space boundary value problems simultaneously. The equations for these problems are nonlinear partial differential equations.
2. The basic boundary condition for fluid surfaces at constant pressure is nonlinear and the function resulting from some finite difference approximations to this boundary condition equation is multivalued in the close vicinity of the zero sought.
3. The three basic inverse partial differential equations contain only first derivatives and products thereof, and therefore iterative methods for solving the resulting finite difference equations are nonconvergent if second or higher order difference approximations are used. The alternatives which have been developed for obtaining a finite difference solution are either to first combine the basic equations to obtain second order quasi-separate equations for each dependent variable x, y and z as done in the previous project report (15) before differencing, or as is done herein to combine solutions obtained from all combinations of first order forward and backward difference approximations to the derivatives in the original three basic equations. Neither approach is completely satisfying.

Other limitations exist which are common to finite difference methods in general. The finite differences approximate the continuous variables poorly in the immediate vicinity of singularities, necessitating either subdividing to a closely spaced grid network or seeking other ad hoc remedies such as "patching in an analytic expression," all of which require quite lengthy computer programming logic.

Other draw-backs are illustrated by the problem of flow about a body described in this report in which the body is to be placed very near the surface. At least two ψ-constant stream surfaces must exist between the body

and the free surface (four ψ-constant surfaces including boundaries) so that the derivatives required by the solution process can be appropriately evaluated. With this restriction the body can be placed very near the surface only if a very small spacing between grid points is used. Thus either a large number of grid points or a variable spacing of grid points must be used. A reduction of the grid spacing by one-half creates $2^3 = 8$ times as many finite difference grid points. Couple this increase in number of grid points with the reduction in convergence rate which occurs and many times as much computer time is required for a solution.

The advantages seem to far outweigh the disadvantages. It is hoped that as others examine the potential role that the inverse formulation can play in solving a variety of fully three-dimensional flow problems with free and cavity surfaces, that the present disadvantages will disappear as more satisfactory means are developed and used in solving the inverse boundary value problems.

RESULTS FROM SOLUTIONS TO THREE-DIMENSIONAL FREE SURFACE FLOWS ABOUT BODIES

The results to four problems with different specifications are presented in this section. The first problem consists of a symmetrically shaped body placed at the center of a flow confined within a rectangular conduit. The second problem is solved also using the same confining conduit, but the body is placed closer to the top boundary than to the bottom. The specifications for the third problem are identical to those of the second problem except a free surface is present. The fourth problem is similar to the third except the body is positioned closer to the free surface in an attempt to obtain more free surface distortion. All four problems were solved in a rectangular channel or conduit with total dimensionless hydraulic head h=1.05 (h=H/W), dimensionless depth of incoming flow d = 1.00 (d=D/W), and dimensionless width of channel w = 1.00 (w = W/W). By using dimensionless variables, the solutions obtained can be applied to bodies in rectangular channels of any size if the dimensionless ratios are maintained. The values read from data cards in the computer program are the actual dimensions (in feet) of the channel and the total hydraulic head. The dimensional values used in all four problems were H=10.5', D=10.0', and W=10.0'. With these values specified, the upstream uniform flow velocity is V_o = 5.69 fps and the flow rate is Q=569 cfs.

Problem No. 1

Eleven equipotential surfaces, nine ψ constant stream surfaces, and nine ψ^* constant stream surfaces were utilized in the finite difference network in solving the first problem. The upstream and downstream stagnation points on the body were specified at the fourth and eighth equipotential surfaces, respectively. The body was enveloped by the fifth ψ constant stream surface and the fifth ψ^* constant stream surface. Using previously defined symbols, the problem specifications are: NP=11, NS=9, NSS=9, LB=4, LN=8, MB=5, and NB=5.

The values of the deviations from the stagnation values of y and z along the different paths along the body surface are given in Table 3. These deviations define the basic shape of the body.

Both y and z at the upstream and downstream stagnation points were equated to 0.5 and x at the sixth equipotential surface was equated to $x_f/2$ because the body was symmetrically placed in the flow field.

The flow nets for two ψ^* constant surfaces in the $\phi\psi\psi^*$ space are shown in Figure 12. This figure represents the projection of the three-dimensional ψ^* constant surfaces onto a vertical plane parallel to the channel sides. For symmetric flow in the z-direction, the ψ^* constant surface of Figure 12 with K=5 becomes a plane surface. The first of these surfaces contains the body and the second is the surface adjacent to the body. The other ψ^* constant surfaces in the solution are not influenced noticeably by the body.

The solution was obtained by specifying uniform flow values for the initial values of x, y, and z at each grid point. Fifteen iterations and three adjustments to the variables on the body surface were needed to obtain the final solution. Full advantage of the symmetric placement of the body in the flow field was taken by specifying some of the variables, which were mentioned previously, and this reduced the computer time needed to obtain a

Table 3. Deviations of y and z from the upstream stagnation values of y and z; these deviations define the body cross section at each equipotential surface along each NUM path for problem 1.

I	NUM	1	2	3	4	5	6	7	8
	5	.070711	.050000	.000000	-.050000	-.070711	-.050000	.000000	.050000
y	6	.100000	.070711	.000000	-.070711	-.100000	-.070711	.000000	.070711
	7	.070711	.050000	.000000	-.050000	-.070711	-.050000	.000000	.050000
	5	.000000	-.050000	-.070711	-.050000	.000000	.050000	.070711	.050000
z	6	.000000	-.070711	-.100000	-.070711	.000000	.070711	.100000	.070711
	7	.000000	-.050000	-.070711	-.050000	.000000	.050000	.070711	.050000

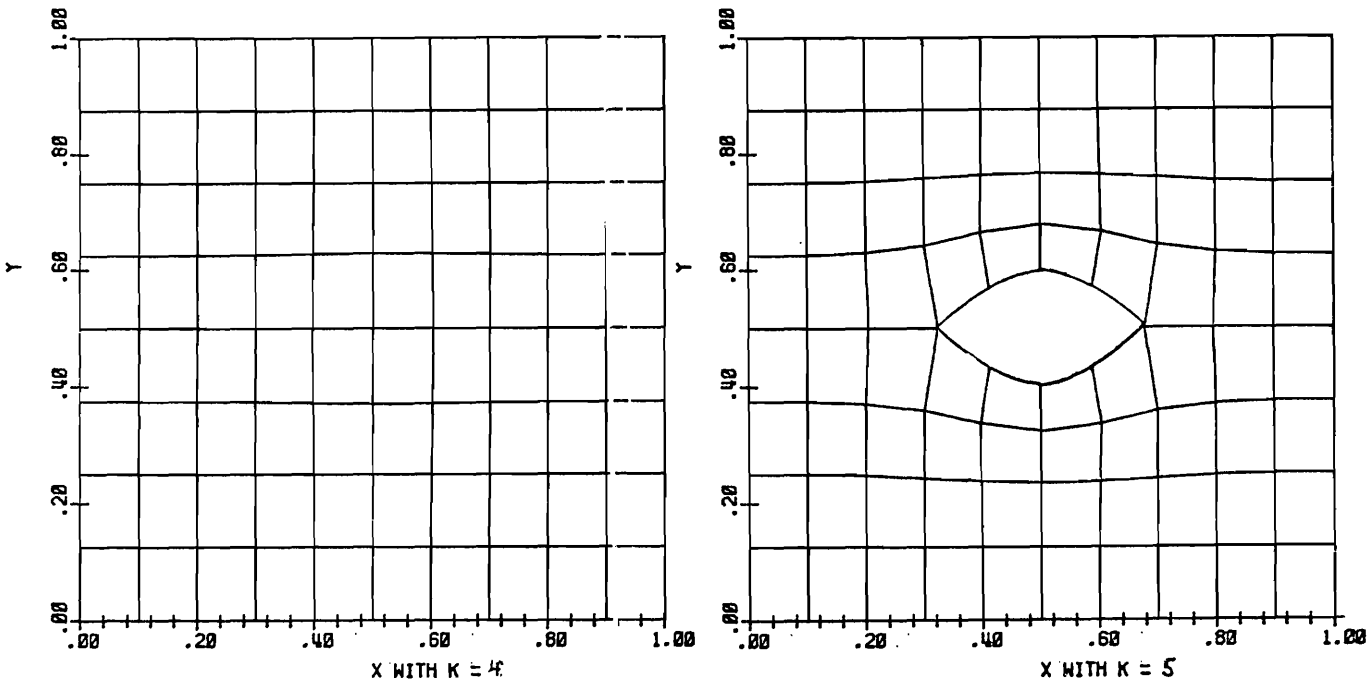

(a) (b)

Figure 12. Flow nets for k constant surfaces described in Problem 1.

solution considerably. Each succeeding value of SUM, which is the sum of the absolute values of the differences in the variables x, y, and z between the previous and the present iteration, was approximately 0.6 times SUM from the previous iteration.

The dimensionless elevation, velocity, and pressure heads and the dimensionless velocity at several points around the body (see Figure 12) are given in Table 4.

Table 4. The dimensionless components of the Bernoulli equation and the dimensionless velocity at several points around the body specified in problem 1. (see Figure 12.)

Point	y=Y/W	$V^2/(2gW)$	$P/(\gamma W)$	V/V_o
1	0.50	0.00	0.55	0.00
2	0.57	0.05	0.43	0.99
3	0.60	0.06	0.39	1.13
4	0.57	0.05	0.43	0.99
5	0.50	0.00	0.55	0.00
6	0.43	0.05	0.57	0.99
7	0.40	0.06	0.59	1.13
8	0.43	0.05	0.57	0.99

Problem No. 2

Specifications for the second problem are: NP=15, NS=11, NSS=11, LB=5, LN=11, MB=7, and NB=6. The y and z deviations from the forward stagnation point are given in Table 5.

The flow net for the ψ^* constant surface that encloses the body and the ψ^* constant surface adjacent to the enclosing surface are shown in Figure 13. The surfaces plotted in Figure 13 actually have varying z- coordinates at each grid point making them three-dimensional surfaces. The influence of the body does not noticeably alter the flow nets in surfaces more remote than those shown.

Each iteration required approximately 5.5 seconds of execution time on the UNIVAC 1108 at the University of Utah Computer Center. The problem was solved by doing a few iterations, examining the results, making changes in the program, doing a few more iterations, and repeating the process. It is estimated that 30 iterations and 4 adjustments to the variables around the body would be required to obtain the solution presented in this report from a uniform flow initialization using the final version of the computer program. The final SUM=0.0215, and the rate of convergence was approximately $SUM_{t+1} = (SUM_t)$ (0.83), in which the subscript t denotes the iteration number. However, the rate of convergence is not constant throughout the solution process; convergence is more rapid when SUM is large.

Table 5. Deviations of y and z from the upstream stagnation values of y and z; these deviations define the body cross section at each equipotential surface along each NUM path for problems 2, 3, and 4.

I	NUM	1	2	3	4	5	6	7	8
	6	.070711	.050000	.000000	-.050000	-.070711	-.050000	.000000	.050000
	7	.100000	.070711	.000000	-.070711	-.100000	-.070711	.000000	.070711
y	8	.110000	.077782	.000000	-.077782	-.110000	-.077782	.000000	.077782
	9	.100000	.070711	.000000	-.070711	-.100000	-.070711	.000000	.070711
	10	.070711	.050000	.000000	-.050000	-.070711	-.050000	.000000	.050000
	6	.000000	-.050000	-.070711	-.050000	.000000	.050000	.070711	.050000
	7	.000000	-.070711	-.100000	-.070711	.000000	.070711	.100000	.070711
z	8	.000000	-.077782	-.110000	-.077782	.000000	.077782	.110000	.077782
	9	.000000	-.070711	-.100000	-.070711	.000000	.070711	.100000	.070711
	10	.000000	-.050000	-.070711	-.050000	.000000	.050000	.070711	.050000

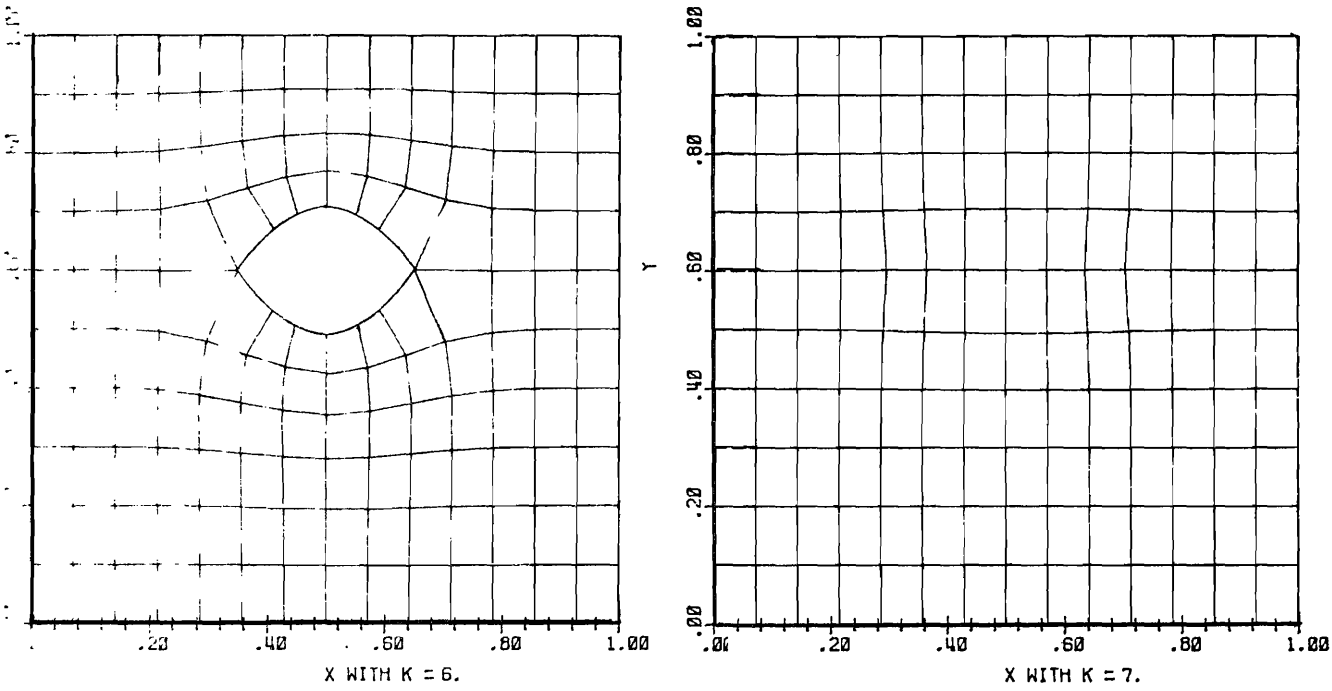

Figure 13. Flow nets for k constant surfaces described in Problem 2.

Problem No. 3

Problem 3 has the same specifications as problem 2 except a free surface is present. Flow nets for the sixth, seventh, and eighth ψ^* constant surfaces are shown in Figure 14. The free surface is influenced only slightly by the relatively small body at the depth and Froude number that exist. The Froude number is defined as

$$F_r = V_o/\sqrt{gY_o} \quad \ldots\ldots\ldots\ldots\ldots \quad (122)$$

The velocity and pressure distributions around the body, as well as the rate of convergence of the solutions, were similar for problems 2 and 3. Since the problem specifications were identical, and the free surface effect was not significant in problem 3, similar solutions are to be expected.

Laboratory tests were conducted in a glass walled, rectangular tilting flume of 1 foot width to determine the effect a small object placed in the flow had on the free surface. The object, which was a small toy football, was placed midway between the channel walls. The flow rate and slope of the flume were adjusted to produce uniform flow of one foot depth at a Froude number equal to that of the computer program (F_r = 0.316). The depth of the object was varied, as shown in Figure 15, but no influence

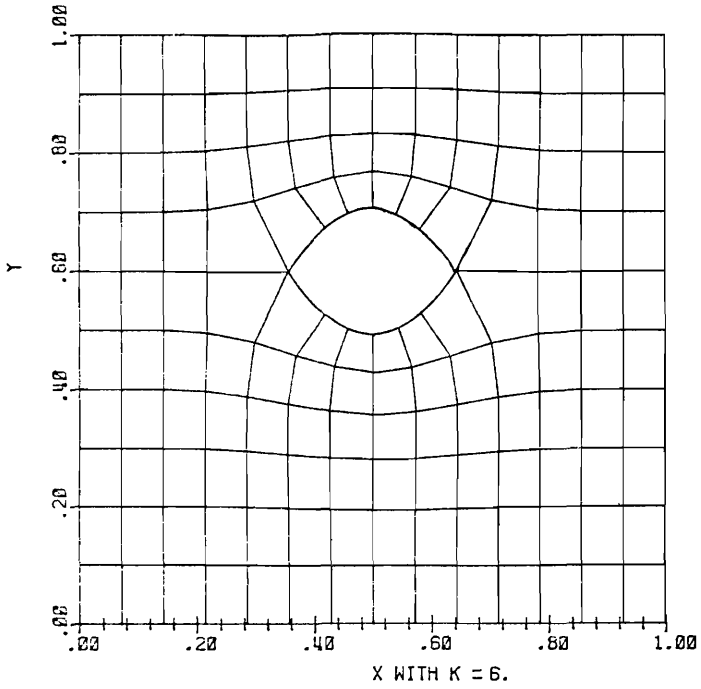

(a)

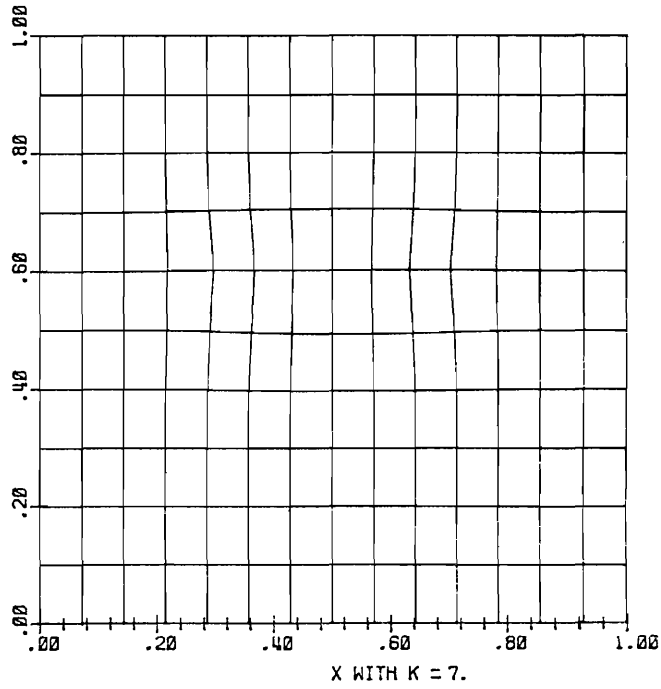

(b)

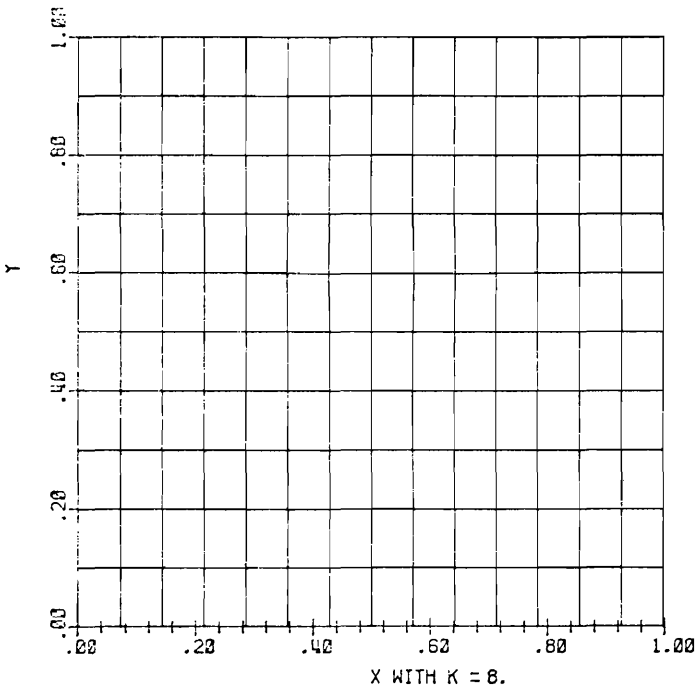

(c)

Figure 14. Flow nets for k constant surfaces described in Problem 3.

on the free surface from the body was noted until the top of the object was less than approximately 0.1 ft deep. A cone of depression immediately behind the top of the body developed when the body was placed near the free surface (see Figure 15b), but little free surface effect at the channel walls was noted. These laboratory observations collaborate the findings of the numerical solutions regarding the small influence the body has on the free surface position when it is at some depth below the surface.

The dimensionless elevation, velocity and pressure heads, and the dimensionless velocity at each equipotential surface that intersects the body in Figure 14 are given in Table 6 for problems 2 and 3.

Problem No. 4

The fourth problem is similar to the third except additional ψ constant surfaces are included to allow the body to be positioned nearer the free surface. The problem specifications are: NP=15, NS=15, NSS=11, MB=11, NB=6, LB=5, LN=11. The y and z deviations from the upstream stagnation point are identical to those shown in Table 5. The flow nets for the ψ^* constant surfaces from the body to the channel wall are shown in Figure 16. The body is not symmetric with respect to x and y although the specified deviations are symmetric, because the x-variables along each NUM path are unequal at each equipotential surface. Additional equipotential surfaces downstream from the body would improve the

(a)

Figure 15. (a) Free surface nearly unchanged by the presence of the body.

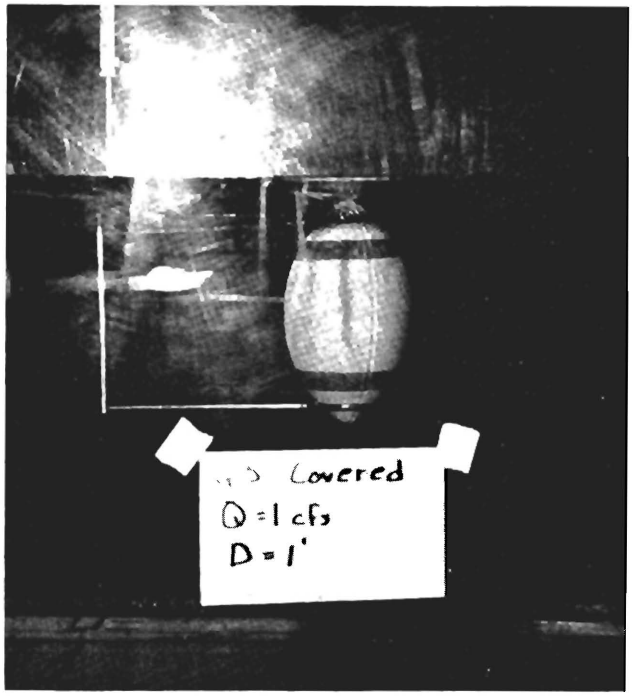

(b)

Figure 15. (b) Free surface affected by the body when the body is placed near the free surface.

Table 6. Dimensionless elevation, velocity, and pressure heads and the dimensionless velocity at various points (see Figure 14) around the body of problems 2 and 3.

Point	y=Y/W	$V^2/(2gW)$	$P/(\gamma W)$	V/V_o
1	0.599	0.000	0.451	0.00
2	0.670	0.051	0.329	1.02
3	0.699	0.133	0.218	1.63
4	0.709	0.138	0.203	1.66
5	0.699	0.130	0.221	1.61
6	0.670	0.051	0.329	1.00
7	0.599	0.000	0.451	0.00
8	0.529	0.051	0.470	1.01
9	0.499	0.128	0.423	1.59
10	0.489	0.133	0.428	1.63
11	0.499	0.127	0.424	1.59
12	0.529	0.051	0.470	1.01

solution, because noticeable deviations from uniform flow exist at the NP1 equipotential surface, particularly on the free surface.

Approximately 40 iterations were needed to obtain the final solution from a uniform flow initialization, with adjustments on the free surface and body being done three times.

The dimensionless elevation, velocity, and pressure heads and the dimensionless velocity at each equipotential surface along NUM paths 1 and 3 on the body (see Figure 16) are given in Table 7.

Table 7. Dimensionless elevation, velocity, and pressure heads and dimensionless velocity at various points (see Figure 16) around the body of problem 4.

Point	y=Y/W	$V^2/(2gW)$	$P/(\gamma W)$	V/V_o
1	0.715	0.000	0.335	0.00
2	0.786	0.055	0.209	1.05
3	0.815	0.168	0.067	1.85
4	0.825	0.144	0.081	1.69
5	0.815	0.151	0.084	1.74
6	0.786	0.142	0.122	1.70
7	0.731	0.000	0.319	0.00
8	0.644	0.057	0.349	1.06
9	0.615	0.252	0.183	2.24
10	0.605	0.180	0.265	1.89
11	0.615	0.127	0.308	1.59
12	0.644	0.044	0.362	0.95

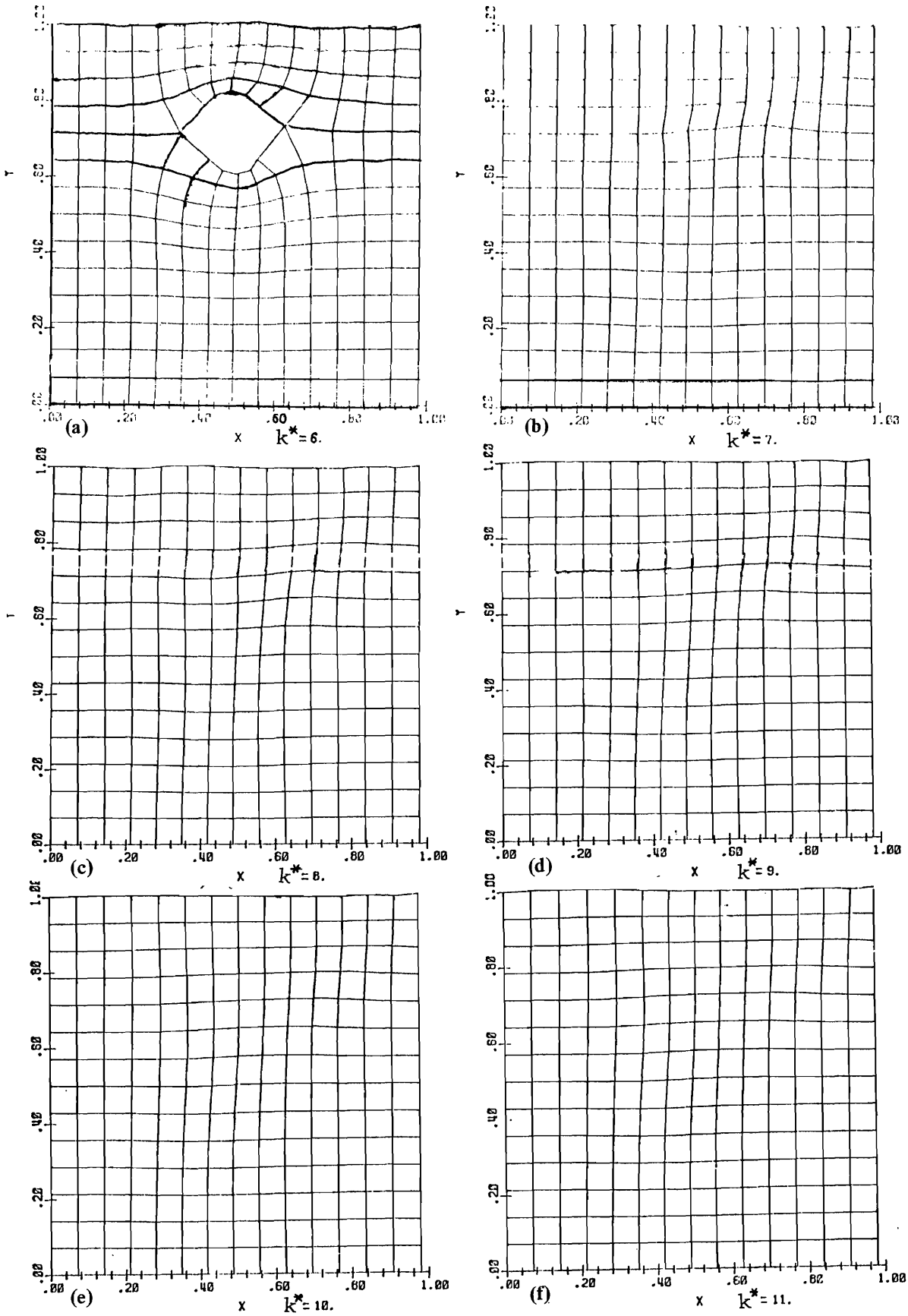

Figure 16. Projections of flow nets for k constant surfaces 6-11 onto a vertical plane.

CONCLUSIONS

The finite difference methods used in this report represent a convergent procedure for solving simultaneously the three inverse, nonlinear, partial differential equations that describe three-dimensional potential flows. These inverse equations are derived by changing the conventional roles played by the variables of the problem, i.e., the magnitudes of the Cartesian coordinates x, y, and z are considered dependent variables while the potential function and two orthogonal stream surface functions are considered the independent variables. A major advantage of the inverse formulation is that free surfaces or cavity surfaces, with unknown positions in the physical space, become planes of known position in this inverse space. Consequently, trial and error adjustments to the positions of such boundaries are unnecessary.

By using high speed digital computers, solutions for potential flows around bodies are practical. The amount of computer time required to obtain a solution depends on the number of grid points and the initialization used and the accuracy required of the solution.

The principal objectives of this study were to develop methods that can be used for solving the inverse equations with a body present in the flow field. The methods were applied to a limited number of flow situations, but the capability to obtain solutions for bodies of any shape is present.

The problems examined in this report might broadly be classified as analysis problems. The method of formulation used is actually better adapted to design type problems by virtue of the fact that the potential function and stream functions are considered the independent variables. In analysis problems the solution is used to describe the flow characteristics caused by known physical boundaries or objects. Design problems are concerned with the shapes or configuration of boundaries which will produce some desired flow characteristics. For example in a design problem the shape of boundary or object which will produce some specified velocity or pressure distribution along its surface may be desired.

For these types of design problems, the boundary of the object of unknown shape is defined by a constant stream surface, that is ψ or ψ^* is constant. From the viewpoint of making the solution as readily attainable as possible, the condition along such a boundary would specify known values for some combination of x and y, x and z, or y and z as a function of the potential function and the other stream function which varies along the boundary. Alternatively, the velocity (or pressure) may be specified as a function of ϕ and ψ or ϕ and ψ^*, and a finite difference operator developed in much the same manner as the operator for the free surface (which is for a zero pressure) to yield the shape needed to produce the given velocity distribution. This shape would be given by values of x, y, and z as functions of ϕ and ψ or ϕ and ψ^* depending respectively if the boundary is defined by a ψ^* or ψ constant stream surface.

Only for problems in which the flow is sufficiently three-dimensional that a two-dimensional solution is inadequate would the methods described in this report be used. Should the flow be completely defined, even though fully three-dimensional, then a solution can more readily be obtained by considering the potential function $\phi(x,y,z)$ the dependent variable in the physical space. When free surfaces and cavities are present (with or without gravity), or if design of boundary shapes are to be determined which will produce a desired flow characteristic, then the inverse formulation and solution method described herein should be considered.

The least satisfying part of this report is the method finally resorted to in order to obtain the numerical solutions. The writers believe a more satisfactory method (or methods) must exist for solving the space boundary value problems associated with three simultaneous, nonlinear partial differential equations. Hopefully, as others examine the merits of the inverse formulation, better numerical solution schemes will be proposed. With improved schemes of solution, the writers believe the inverse formulation approach will find wide application in obtaining approximate solutions to fully three-dimensional potential problems.

REFERENCES

1. Ames, W.F. Nonlinear partial differential equations in engineering. Academic Press, New York, N.Y., 1965.

2. Birkhoff, Garrett and E. H. Zarantonello. Jets, wakes, and cavities. Academic Press, New York, N.Y., 1957.

3. Carnahan, Brice, H. A. Luther, and James O. Wilkes. Applied numerical methods. John Wiley & Sons, New York, N.Y., 1969.

4. Cassidy, J. J. Irrotational flow over spillways of finite height. Journal of the Engineering Mechanics Division, ASCE, Vol. 91, No. EM6, Proc. Paper 4581, December 1965, pp. 155-174.

5. Draper, N. R. and H. Smith. Applied regression analysis. John Wiley & Sons, New York, N.Y., 1966.

6. Finnemore, E. J. and B. Perry. Seepage through an earth dam computed by the relaxation technique. Water Resources Research, Vol. 4, No. 5, October, 1968, pp. 1059-1067.

7. Forsythe, George E. and Wolfgang R. Wasow. Finite-difference methods for partial differential equations. John Wiley & Sons, New York, N.Y., 1967.

8. Fox, Leslie. Numerical solution of ordinary and partial differential equations. Pergamon Press, Oxford, England, 1962.

9. Gilbarg, D. Jets and cavities. Handbuck der Physik, Vol. IX, Springer-Verlag, Berlin, Germany, 1960.

10. Gurevich, M. L. Theory of jets in ideal fluids. Translated from Russian by R. L. Street and K. Zagustin, Academic Press, New York, N.Y., 1965.

11. Hamming, Richard W. Introduction to applied numerical analysis. McGraw-Hill Book Co., New York, N.Y., 1971.

12. Jeppson, Roland W. Numerical solutions to free-surface axisymmetric flows. Journal of the Engineering Mechanics Division, ASCE, Vol. 95, No. EM1, Proc. Paper 6381, February, 1969, pp. 1-20.

13. Jeppson, Roland W. Inverse formulation and finite difference solution for flow from a circular orifice. Journal of Fluid Mechanics, Vol. 40, Part 1, 1970, pp. 215-223.

14. Jeppson, Roland W. Free streamline problems solved by inverse formulation and finite differences. Developments in Mechanics, Vol. 5, Iowa State University Press, Ames, Iowa, 1969.

15. Jeppson, Roland W. Studies to develop and investigate an inverse formulation for numerically solving three-dimensional free surface potential fluid flows. PRWG-96-1, Utah Water Research Laboratory, Utah State University, Logan, Utah, May, 1972.

16. Jeppson, Roland W. Inverse solution to three-dimensional potential flows. Journal of the Engineering Mechanics Division, ASCE, Vol. 98, No. EM4, Proc. Paper 9110, August, 1972, pp. 789-812.

17. Markland, E. Calculation of flow at a free overfall by relaxation method. Proceedings, Institution of Civil Engineers, Vol. 31, May, 1965, pp. 71-79.

18. McNown, J. S., Y. Hsu, and C. S. Yih. Applications of the relaxation technique in fluid mechanics. Transaction, ASCE, Vol. 79, 1953, pp. 223-248.

19. Protter, Murray H. and Charles B. Morrey, Jr. Modern mathematical analysis. Addison-Wesley Publishing Co., Reading, Mass., 1964.

20. Rouse, H. and A. Abul-Fetouh. Characteristics of irrotational flow through axially symmetric orifice. Journal of Applied Mechanics, Vol. 17, No. 4, 1950, pp. 421-426.

21. Southwell, R. V. and G. Vaisey. Relaxation methods applied to engineering problems, XII fluid motions characterized by free streamlines. Philosophical Transactions of the Royal Society of London, Series A, Vol. 240, 1948, pp. 117-161.

22. Taylor, Angus E. Advanced calculus. Ginn and Co., New York, N.Y., 1955.

23. Thurnau, Donald H. Algorithm 195, BANDSOLVE. Association for Computing Machinery, Vol. 6, No. 8, August, 1963, pp. 441.

24. Varga, Richard S. Matrix iterative analysis. Prentice-Hall, Inc., Englewood Cliffs, N.J., 1962.

25. Wilde, Douglas J. and Charles S. Beightler. Foundations of optimization. Prentice-Hall, Inc., Englewood Cliffs, N.J., 1967.

26. Wilson, L.B. Solution of certain large sets of equations on Pegasus using matrix methods. Computer J., Vol. 2, pp. 130-133.

27. Yih, C. S. Stream functions in three-dimensional flows. LaHouille Blanche, Vol. 12, No. 3, 1957, pp. 445-450.

Unclassified
Security Classification

DOCUMENT CONTROL DATA - R & D

(Security classification of title, body of abstract and indexing annotation must be entered when the overall report is classified)

1. ORIGINATING ACTIVITY (Corporate author)	2a. REPORT SECURITY CLASSIFICATION
Utah Water Research Laboratory Utah State University Logan, Utah 84322	Unclassified 2b. GROUP

3 REPORT TITLE

SOLVING THREE-DIMENSIONAL POTENTIAL FLOW PROBLEMS BY MEANS OF AN INVERSE FORMULATION AND FINITE DIFFERENCES

4. DESCRIPTIVE NOTES *(Type of report and inclusive dates)*

5. AUTHOR(S) *(First name, middle initial, last name)*

Allen L. Davis
Roland W. Jeppson

6. REPORT DATE	7a. TOTAL NO. OF PAGES	7b. NO. OF REFS
March 1973	41	27

8a. CONTRACT OR GRANT NO.	9a. ORIGINATOR'S REPORT NUMBER(S)
N00014-67-A-0220-0003 b. PROJECT NO. SR 009 01 01 c. Naval Ship Systems Command d. General Hydromechanics Research Prog.	PRWG-96-2 9b. OTHER REPORT NO(S) *(Any other numbers that may be assigned this report)*

10. DISTRIBUTION STATEMENT

This document has been approved for public release and sale; its distribution is unlimited

11. SUPPLEMENTARY NOTES	12. SPONSORING MILITARY ACTIVITY
	Naval Ship Research and Development Center Department of the Navy Bethesda, Maryland 20034

13. ABSTRACT

A finite difference method is developed to solve the three-dimensional, steady, incompressible, potential flow equations obtained by using a potential function, ϕ, and two mutually orthogonal stream functions, ψ and ψ^*, to describe the flow. Problems are formulated in an inverse space where the potential function and the two stream functions are the independent variables, and the Cartesian coordinates x, y, and z are the dependent variables. The boundaries of the problem in the physical space, including the free surface, have known positions in the inverse space, so trial and error adjustments to the positions of the boundaries are unnecessary.

Methods of describing the effect of the placement of a body, whose shape is partially specified, in the flow field are developed using finite differences, and a solution for the x-, y-, and z-coordinates is obtained at each grid point formed by the intersection of surfaces held constant with respect to ϕ, ψ, and ψ^* in the inverse space.

14 KEY WORDS	LINK A		LINK B		LINK C	
	ROLE	WT	ROLE	WT	ROLE	WT
Inviscid flow						
Three-dimensional						
Numerical solution						
Free Surface gravity						
Inverse formulation						

40 Commander
Naval Ship Research and
Development Center
Bethesda, Maryland 20034
Attn: Code 1505
Code 5614 (39 cys)

1 Officer-in-Charge
Annapolis Laboratory
Naval Ship Research and
Development Center
Annapolis, Maryland 21402
Attn: Code 5642(Library)

6 Commander
Naval Ship Systems Command
Washington, D. C. 20360
Attn: SHIPS 2052 (3 cys)
SHIPS 03412B
SHIPS 0372
SHIPS 0342

12 Director
Defense Documentation Center
5010 Duke Street
Alexandria, Virginia 22314

1 Office of Naval Research
800 N. Quincy Street
Arlington, Virginia 22217
Attn: Mr. R. D. Cooper (Code 438)

1 Office of Naval Research
Branch Office
492 Summer Street
Boston, Mass 02210

1 Office of Naval Research
Branch Office (493)
536 S. Clark Street
Chicago, Illinois 60605

1 Chief Scientist
Office of Naval Research
Branch Office
1030 E. Green Street
Pasadena, CA 91106

1 Office of Naval Research
Resident Representative
207 West 24th Street
New York, New York 10011

1 Office of Naval Research
Resident Representative
50 Fell Street
San Francisco, CA 94102

2 Director
Naval Research Laboratory
Washington, D. C. 20390
Attn: Code 2027
Code 2629(ONRL)

1 Commander
Naval Facilities Engineering
Command(Code 032C)
Washington, D. C. 20390

1 Library of Congress
Science & Technology Division
Washington, D. C. 20540

1 Commander
Naval Ordnance Systems
Command (ORD 035)
Washington, D. C. 20360

1 Commander
Naval Electronics Laboratory
Center (Library)
San Diego, CA 92152

8 Commander
Naval Ship Engineering Center
Center Building
Prince Georges Center
Hyattsville, Maryland 20782
Attn: SEC 6034B
SEC 6110
SEC 6114H
SEC 6120
SEC 6136
SEC 6144G
SEC 6140B
SEC 6148

1 Naval Ship Engineering Center
Norfolk Division
Small Craft Engr Dept
Norfolk, Virginia 23511
Attn: D. Blount (6660.03)

1 Library (Code 1640)
Naval Oceanographic Office
Washington, D. C. 20390

1 Technical Library
Naval Proving Ground
Dehlgren, Virginia 22448

1 Commander (ADL)
Naval Air Development Center
Warminster, Penna 18974

1 Commanding Officer (L31)
Naval Civil Engineering Laboratory
Port Hueneme, CA 93043

1 Commander
Naval Undersea Center
San Diego, CA 92132
Attn: Dr. A. Fabula (6005)

2 Officer-in-Charge
Naval Undersea Center
Pasadena, CA 91107
Attn: Dr. J. Hoyt (2501)
Library (13111)

1 Director
Naval Research Laboratory
Underwater Sound Reference Division
P.O. Box 8337
Orlando, Florida 32806

1 Library
Naval Underwater Systems Center
Newport, R. I. 02840

1 Research Center Library
Waterways Experiment Station
Corp of Engineers
P.O. Box 631
Vicksburg, Mississippi 39180

2 National Bureau of Standards
Washington, D. C. 20234
Attn: P. Klebanoff (FM 105)
Fluid Mechanics
Hydraulic Section

1 AFOSR/NAM
1400 Wilson Blvd
Arlington, Virginia 22209

1 AFFOL/FYS (J. Olsen)
Wright Patterson AFB
Dayton, Ohio 45433

1 Dept. of Transportation
Library TAD-491.1
400 - 7th Street S.W.
Washington, D. C. 20590

1 Boston Naval Shipyard
Planning Dept Bldg 39
Technical Library, Code 202.2
Boston, Mass 02129

1 Charleston Naval Shipyard
Technical Library
Naval Base
Charleston, S. C. 29408

1 Norfolk Naval Shipyard
Technical Library
Portsmouth, Virginia 23709

1 Philadelphia Naval Shipyard
Philadelphia, Penna 19112
Attn: Code 240

1 Portsmouth Naval Shipyard
Technical Library
Portsmouth, N. H. 03801

1 Puget Sound Naval Shipyard
Engineering Library
Bremerton, Wash 98314

1 Long Beach Naval Shipyard
Technical Library (246L)
Long Beach, CA 90801

1 Hunters Point Naval Shipyard
Technical Library (Code 202.3)
San Francisco, CA 94135

1 Pearl Harbor Naval Shipyard
Code 202.32
Box 400, FPO
San Francisco, CA 96610

1 Mare Island Naval Shipyard
Shipyard Technical Library
Code 202.3
Vallejo, CA 94592

1 Assistant Chief Design Engineer
for Naval Architecture (Code 250)
Mare Island Naval Shipyard
Vallejo, CA 94592

3 U. S. Naval Academy
Annapolis, Maryland 21402
Attn: Technical Library
Dr. Bruce Johnson
Prof. P. Van Mater, Jr.

3 Naval Postgraduate School
Monterey, CA 93940
Attn: Library, Code 2124
Dr. T. Sarpkaya
Prof. J. Miller

1 Capt. L. S. McCready, USMS
Director, National Maritime
Research Center
U. S. Merchant Marine Academy
Kings Point, L.I., N.Y. 11204

1 U. S. Merchant Marine Academy
Kings Point, L.I., N.Y. 11204
Attn: Academy Library

1 Library
The Pennsylvania State University
Ordnance Research Laboratory
P. O. Box 30
State College, Penna 16801

1 Bolt, Beranek & Newman
1501 Wilson Blvd
Arlington, Virginia 22209
Attn: Dr. F. Jackson

1 Bolt, Beranek & Newman
50 Moulton Street
Cambridge, Mass 02138
Attn: Library

1 Bethlehem Steel Corporation
Center Technical Division
Sparrows Point Yard
Sparrows Point, Maryland 21219

1 Bethlehem Steel Corporation
25 Broadway
New York, New York 10004
Attn: Library (Shipbuilding)

1 Cambridge Acoustical Associates, Inc.
1033 Mass Avenue
Cambridge, Mass 02138
Attn: Dr. M. Junger

1 Cornell Aeronautical Laboratory
Aerodynamic Research Dept.
P.O. Box 235
Buffalo, N.Y. 14221
Attn: Dr. A. Ritter

1 Eastern Research Group
P.O. Box 222
Church Street Station
New York, New York 10008

1 Esso International
Design Division, Tanker Dept.
15 West 51st Street
New York, New York 10019

1 Mr. V. Boatwright, Jr.
R & D Manager
Electric Boat Division
General Dynamics Corporation
Groton, Conn 06340

1 Gibbs & Cox, Inc.
21 West Street
New York, New York 10006
Attn: Technical Info. Control

1 Hydronautics, Inc.
Pindell School Road
Howard County
Laurel, Maryland 20810
Attn: Library

2 McDonnell Douglas Aircraft Co.
3855 Lakewood Blvd
Long Beach, CA 90801
Attn: J. Hess
A.M.O. Smith

1 Lockheed Missiles & Space Co.
P.O. Box 504
Sunnyvale, CA 94088
Attn: Mr. R. L. Waid, Dept 57-74
Bldg. 150, Facility 1

1 Newport News Shipbuilding &
Dry Dock Company
4101 Washington Avenue
Newport News, Virginia 23607
Attn: Technical Library Dept.

1 North American Aviation, Inc.
Space & Information Systems Div.
12214 Lakewood Blvd
Downey, CA 90241
Attn: Mr. Ben Ujihara (SL-20)

1 Nielsen Engineering & Research, Inc.
850 Maude Avenue
Mountain View, CA 94040
Attn: Mr. S. B. Spangler

1 Oceanics, Inc.
Technical Industrial Park
Plainview, L.I., N.Y. 11803

1 Society of Naval Architects
and Marine Engineers
74 Trinity Place
New York, New York 10006
Attn: Technical Library

1 Sperry Systems Management Division
Sperry Rand Corporation
Great Neck, N. Y. 11020
Attn: Technical Library

1 Stanford Research Institute
Menlo Park, CA 94025
Attn: Library G-021

2 Southwest Research Institute
P. O. Drawer 28510
San Antonio, Texas 78284
Attn: Applied Mechanics Review
Dr. H. Abramson

1 Tracor, Inc.
6500 Tracor Lane
Austin, Texas 78721

1 Mr. Robert Taggart
3930 Walnut Street
Fairfax, Virginia 22030

1 Ocean Engr Department
Woods Hole Oceanographic Inst.
Woods Hole, Mass 02543

1 Worcester Polytechnic Inst.
Alden Research Laboratories
Worcester, Mass 01609
Attn: Technical Library

1 Applied Physics Laboratory
University of Washington
1013 N. E. 40th Street
Seattle, Washington 98105
Attn: Technical Library

1 University of Bridgeport
Bridgeport, Conn 06602
Attn: Dr. E. Uram

1 Cornell University
Graduate School of Aerospace Engr
Ithaca, New York 14850
Attn: Prof. W. R. Sears

4 University of California
Naval Architecture Department
College of Engineering
Berkeley, CA 94720
Attn: Library
Prof. W. Webster
Prof. J. Paulling
Prof. J. Wehausen

3 California Institute of Technology
Pasadena, CA 91109
Attn: Aeronautics Library
Dr. T. Y. Wu
Dr. A. J. Acosta

1 Docs/Repts/Trans Section
Scripps Institution of
Oceanography Library
University of California, San Diego
P.O. Box 2367
La Jolla, CA 92037

1 Catholic University of America
Washington, D. C. 20017
Attn: Dr. S. Heller, Dept of
Civil & Mech Engr

1 Colorado State University
Foothills Campus
Fort Collins, Colorado 80521
Attn: Reading Room, Engr Res Center

1 University of California at San Diego
La Jolla, CA 92038
Attn: Dr. A. T. Ellis
Dept of Applied Math

2 Harvard University
Pierce Hall
Cambridge, Mass 02138
Attn: Prof. G. Carrier
Gordon McKay Library

1 University of Hawaii
Department of Ocean Engineering
2565 The Mall
Honolulu, Hawaii 96822
Attn: Dr. C. Bretschneider

1 University of Illinois
Urbana, Illinois 61801
Attn: Dr. J. Robertson

3 Institute of Hydraulic Research
The University of Iowa
Iowa City, Iowa 52240
Attn: Library
Dr. L. Landweber
Dr. J. Kennedy

1 The John Hopkins University
Baltimore, Md 21218
Attn: Prof. O. Phillips
Mechanics Dept

1 Kansas State University
Engineering Experiment Station
Seaton Hall
Manhattan, Kansas 66502
Attn: Prof. D. Nesmith

1 University of Kansas
Chm Civil Engr Dept Library
Lawrence, Kansas 60644

1 Fritz Engr Laboratory Library
Depart of Civil Engr
Lehigh University
Bethlehem, Penna 18015

5 Department of Ocean Engineering
Massachusetts Institute of Technology
Cambridge, Mass 02139
Attn: Department Library
Prof. P. Leehey
Prof. P. Mandel
Prof. M. Abkowitz
Dr. J. Newman

1 Parsons Laboratory
Massachusetts Institute of Technology
Cambridge, Mass 02139
Attn: Prof. A. Ippen

5 St. Anthony Falls Hydraulic Laboratory
University of Minnesota
Mississippi River at 3rd Avenue S.E.
Minneapolis, Minnesota 55414
Attn: Director
Mr. J. Wetzel
Mr. F. Schiebe
Mr. J. Killen
Dr. C. Song

3 Department of Naval Architecture
and Marine Engineering
University of Michigan
Ann Arbor, Michigan 48104
Attn: Library
Dr. T. F. Ogilvie
Prof. F. Hammitt

2 College of Engineering
University of Notre Dame
Notre Dame, Indiana 46556
Attn: Engineering Library
Dr. A. Strandhagen

2 New York University
Courant Inst. of Math. Sciences
251 Mercier Street
New York, New York 10012
Attn: Prof. A. Peters
Prof. J. Stoker

New York University
University Heights
Bronx, New York 10453
Attn: Prof. W. Pierson, Jr.

Department of Aerospace &
Mechanical Sciences
Princeton University
Princeton, N.J. 08540
Attn: Prof. G. Mellor

3 Davidson Laboratory
Stevens Institute of Technology
711 Hudson Street
Hoboken, New Jersey 07030
Attn: Library
Mr. J. Breslin
Mr. S. Tsakonas

1 Department of Mathematics
St. John's University
Jamaica, New York 11432
Attn: Prof. J. Lurye

1 Applied Research Laboratory Library
University of Texas
P.O. Box 8029
Austin, Texas 78712

College of Engineering
Utah State University
Logan, Utah 84321
Attn: Dr. R. Jeppson

2 Stanford University
Stanford, CA 94305
Attn: Engineering Library
Dr. R. Street

3 Webb Institute of Naval Architecture
Crescent Beach Road
Glen Cover, L.I., N.Y. 11542
Attn: Library
Prof. E. V. Lewis
Prof. L. W. Ward

1 National Science Foundation
Engineering Division Library
1800 G Street N. W.
Washington, D. C. 20550

1 University of Connecticut
Box U-37
Storrs, Conn 06268
Attn: Dr. V. Scottron
Hydraulic Research Lab

1 Long Island University
Graduate Department of
Marine Science
40 Merrick Avenue
East Meadow, L.I., N.Y. 11554
Attn: Prof. David Price

1 Dr. Douglas E. Humphreys (Code 712)
Naval Coastal Systems Laboratory
Panama City, Florida 32401